Pure Appl. Geophys. 176 (2019), 2425–2449

https://doi.org/10.1007/s00024-018-2083-7

Pure and Applied Geophysics

CrossMark

# Challenges in the Detection of Ionospheric Pre-Earthquake Total Electron Content Anomalies (PETA) for Earthquake Forewarning

B. J. M. Lim[1] and E. C. Leong[2]

*Abstract*—Various studies have investigated the link between seismic activity and ionospheric precursory phenomena. Many of these retrospective case studies have supported the existence of pre-earthquake ionospheric anomalies by examining past earthquake events using a variety of analytical methods. Based on existing methodologies, however, the conversion of a retrospective analysis to a prospective forewarning scenario is not a straightforward process. The obstacles to its potential adoption stem mainly from assumptions made during data analysis and interpretation. In this study, several parameters pertaining to existing approaches for the detection of these ionospheric anomalies are highlighted and discussed, in particular ionosphere total electron content (TEC). A detailed examination is conducted to understand the roles that each of these parameters play in the detection process and the consequent difficulties when adopting them in a prospective analysis. These issues include accounting for variations in ionosphere characteristics owing to different measurement platforms (e.g. ground- and space-based observations) and statistical methods (e.g. standard deviation envelopes) used in detecting anomalies. Furthermore, the necessity of excluding space weather contributions in the underlying TEC fluctuations poses a challenge in determining the validity of observed ionospheric anomalies. The notion of an "earthquake preparation zone" is also evaluated in the context of the ionosphere, along with its implications in a forewarning scenario. These issues need to be addressed in current research in order to enable its possible application in earthquake forewarning.

**Key words:** Earthquakes, precursor, TEC, seismo-ionospheric anomalies, statistical analysis.

## 1. Introduction

Ever since the first reported pre-earthquake ionospheric anomalies on 28 March 1964 (Good Friday Alaska earthquake) by Moore (1964), much interest has been generated within the scientific community regarding the detailed characterization and utilization of these anomalies as earthquake precursors. There is a plethora of literature regarding seismo-ionospheric associations and their coupled nature (e.g. Calais and Minster 1995; Chmyrev et al. 1997; Devi et al. 2014; Hayakawa and Molchanov 2002; Krankowski et al. 2006; Liperovsky et al. 2000; Liu et al. 2006a; Pulinets and Boyarchuk 2004; Zakharenkova et al. 2008; Barkat et al. 2018). These works suggest that perturbations are induced in the upper atmosphere and ionosphere by ground processes that could be recorded by various platforms, such as satellites (Hsiao et al. 2010; Sarkar and Gwal 2010; Zhang et al. 2009), ionosondes (Xu et al. 2010; Yu et al. 2009), ground-based GPS stations (Lin 2010; Yu et al. 2009) and ionospheric maps (Hocke 2008; Mendillo et al. 2005). The origin and reason for such ground processes, known more commonly as "seismic preparation or activation" processes, have also been postulated in various studies. For example, the concept of micro-fracturing effecting the creation and relaxation of charges at crack openings and inductive magnetohydrodynamics have been suggested by Molchanov and Hayakawa (1995), Surkov (1999) and Surkov et al. (2003). The occurrence of radon emissions on days leading to an earthquake was cited as a plausible cause (Pulinets 2004). Studies looking into wave-related origins such as atmospheric gravity, acoustic-gravity waves or direct wave production have also seemed to yield conclusive results (Depueva and Ruzhin 1993; Mareev et al. 2002). Other explanations for such seismo-ionospheric effects include the emanation of warm gases (Hayakawa and Molchanov 2002) and the vertical transport

[1] Satellite Research Centre, Nanyang Technological University, Singapore, Singapore.
[2] School of Civil and Environmental Engineering, Nanyang Technological University, Blk N1, 50 Nanyang Avenue, Singapore 639798, Singapore. E-mail: cecleong@ntu.edu.sg

of F2-region ionosphere plasma (Namgaladze et al. 2009). More recently, the lithosphere–atmosphere–ionosphere coupling model (LAIC) proposed by Pulinets and Ouzounov (2011) and the positive-hole (p-hole) theory by Freund (2000) appear to provide valid fundamental-based justifications for pre-earthquake ionospheric anomaly manifestations. In addition, Reddy et al. (2016) have given detailed explanations on ground chemistry leading to atmospheric electrical conductivity changes during seismic preparation. These varied hypotheses regarding seismic preparation and physical mechanisms behind these anomalies clearly evidence a lack of consensus, and thus remain controversial (Klimenko et al. 2011; Polyakov et al. 2015; Masci et al. 2017). Therefore, until more empirical evidence is presented, the generation of these anomalies is still not well understood, even though their existence has been observed in numerous case studies (Liu et al. 2010a).

Other non-ionospheric earthquake precursors (such as thermal infrared anomalies, earthquake lights or unusual animal behavior) are also reported (Freund et al. 2009; Jordan et al. 2011; Polyakov et al. 2015). Several agencies (e.g. the GeoCosmo team in the USA, PRE-EARTHQUAKES project in Europe, Earthquake Integrated Frontier Research project in Japan, iSTEP project in Taiwan, Iono-Quake system in Indonesia) have embarked on goal-oriented studies to employ multifaceted precursors, data sources (e.g. ground and remote sensing methods) and analytical procedures in order to improve current knowledge regarding pre-earthquake anomaly manifestations and for possible development of an earthquake forewarning system (Tsai et al. 2004). For successful earthquake prediction, the time, location and strength (i.e. when, where, what) of the earthquake must be determined (Jordan et al. 2011; Monroe et al. 2007). In this paper, the term "earthquake forewarning" is preferred over "earthquake prediction", as the reliability, and thus the utility, of earthquake precursors has yet to be ascertained.

The objective of this paper is to examine the challenges associated with the use of ionospheric-based pre-earthquake total electron content anomalies (PETA) for earthquake forewarning. It should be noted that PETA is a subset of the pre-earthquake ionospheric anomaly (PEIA) proposed in the literature (Liu et al. 2006a). Here, the methodologies previously employed in detecting PETA are critically reviewed. Specific issues regarding the use of PETA in earthquake forewarning are outlined and discussed. Finally, suggestions are made for future work on PETA.

## 2. *PETA Case Studies and Challenges*

Using the Clarivate Analytics Web of Science (WoS) scientometrics platform, case studies on earthquake precursors up to 2015 were compiled based on precursor type, and are summarized in Fig. 1 (Clarivate Analytics 2017; Li et al. 2018). Here, the list of publications indexed by various keyword combinations, including "earthquake", "seismic", "precursor", "ionosphere", "total electron content", "electromagnetic emissions", "seismo-ionospheric (ionosphere)" and "perturbations", was first filtered for any repeated publications and subsequently classified according to precursor type and quantity. Figure 1 shows that total electron content (TEC) and radon-, thoron- and groundwater-related anomalies were the most widely studied. A comparison of TEC and radon/thoron/groundwater studies in Fig. 2 shows that studies on radon/thoron/groundwater observations were generally more common than those involving ionospheric TEC in the period before and during the early 2000s. This trend is reversed, with a marked increase in ionospheric TEC studies, after 2007.

As with the majority of earthquake precursor studies, PETA case studies are retrospective in nature (i.e. conducted after the event). For example, publications within the past 6 years (e.g. Chauhan et al. 2009; Singh et al. 2009; Liu et al. 2010a; Tojiev et al. 2013; Nenovski et al. 2015; Sánchez-Dulcet et al. 2015) were undertaken based on past significant earthquakes. A search of the database for relevant publications (i.e. seismic effects on TEC) further revealed an overall increasing number of case studies on PETA from 2010 onward. This observation is similarly reflected in Fig. 2. Plausible reasons for the trend may be the increasing availability of TEC data, especially space-based sources such as low-earth

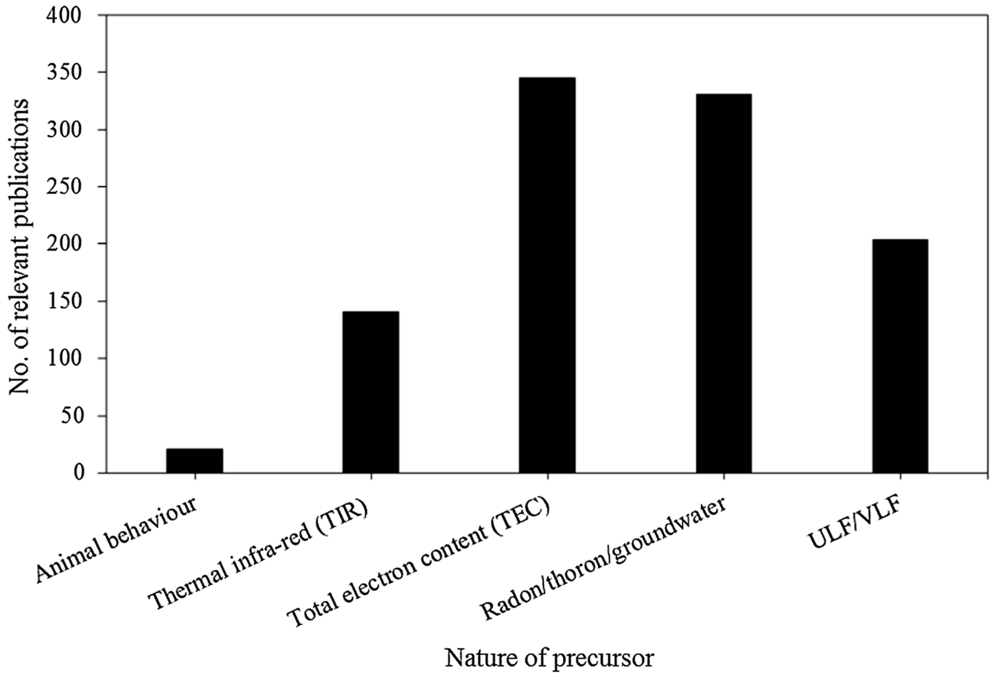


Figure 1
Number of publications classified by nature of precursor

orbiters (LEO) from the European satellite constellation SWARM, the upcoming launch of the US/Taiwan follow-up mission FORMOSAT-7/COSMIC-2, and the near-equatorial orbiter (NEO) climate research satellite VELOX-CI from Singapore. In view of increasing global development and urbanization, it will be very useful to have earthquake forewarning to lessen the impact of earthquakes (Boughazi et al. 2014; Islam et al. 2015).

Figure 2 also shows a gradual decline in earthquake precursory studies from 2012 onward, which may be attributed to a general stagnation of research in this area. In addition, several works have questioned the validity of ionospheric precursors due to misinterpretations regarding the origins of ionospheric anomalies. For example, the TEC anomaly occurring at about 40 min before the 2011 $M_w$ 9.0 Tohoku Japan earthquake presented by Heki (2011) could be caused by a tsunamigenic ionospheric hole rather than a precursory enhancement (Kamogawa and Kakinami 2013). In general, the ionosphere plays host to complex and dynamic electromagnetic interactions such as space weather activity, anthropogenic effects (e.g. missile launches) and meteorological events (e.g. stratospheric sudden warming) (Kakinami et al. 2013; Masci 2012). Among these, it is well known that ionospheric TEC is highly modulated by solar and geomagnetic activity, which exhibits significant inter- (e.g. daily, seasonal) and even intra-day (e.g. hourly) variability (Rishbeth 2006). For instance, Dautermann et al. (2007) found that TEC levels are dominated by the cyclical nature of daily solar fluctuations and lunar tides, giving rise to diurnal and semi-diurnal periodicities. Without accounting for these strong oscillatory phenomena, observations of ionospheric TEC anomalies could be a result of such dynamic space weather interactions. Likewise, Masci et al. (2017) reported the presence of such cycles in what was construed as TEC anomalies in Nenovski et al. (2015). Recently, Thomas et al. (2017) investigated a large global database of 1279 $M \geq 6.0$ earthquakes with corresponding geomagnetic Dst and Kp indices. In contrast to the conclusions presented by Le et al. (2011), Thomas et al. (2017) demonstrated that the TEC anomalies

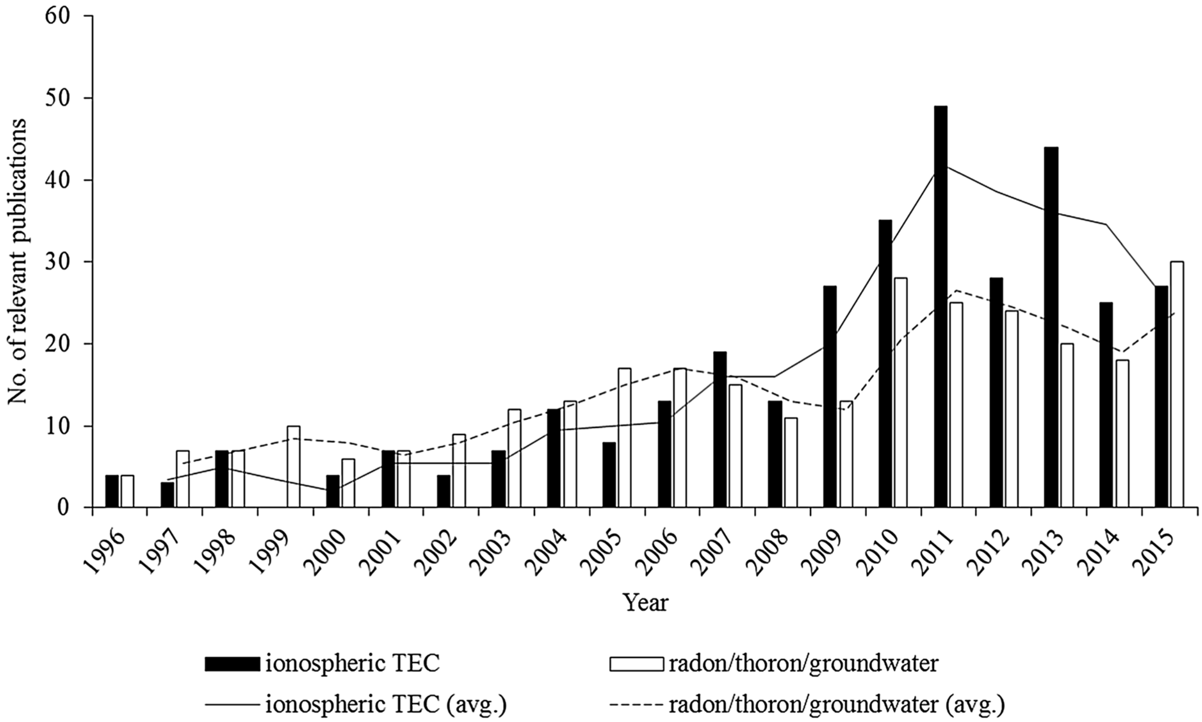


Figure 2
Comparison of number of publications between ionospheric TEC and radon/thoron/groundwater

observed were statistically non-significant relative to the background TEC.

An earlier study conducted by Afraimovich et al. (2008) revealed that the global electron content follows a strong 27-day cycle (mainly due to the sun's ultraviolet radiation and geomagnetic activity), accounting for large changes to the amplitudes of TEC (i.e. up to 20–30% deviations) (Afraimovich and Astafyeva 2008; Astafyeva et al. 2008). The high degree of ionospheric background variability makes it difficult for one to confidently detect terrestrial perturbations at these altitudes. For example, Afraimovich et al. (2004) and Masci (2013) scrutinized TEC (i.e. 1999 Hector Mine earthquake) with concurrent geomagnetic indices (i.e. Kp and Dst) and discovered good correlation between them, proving that the TEC fluctuations could be explained by normal solar-terrestrial interactions. Thomas et al. (2012) reported similar findings in their investigation of the same earthquake using long-term GPS data. The detection of any seismo-ionospheric signatures is thus problematic, since changes in solar flux (e.g. local time variations) and magnetic field intensity (whether periodic oscillations or flare events) could potentially overwhelm these signals (Afraimovich et al. 2004). In light of these studies, it is hence challenging to prove a causal link between TEC anomalies and earthquake occurrence owing to perturbations from space weather.

As such, Fig. 3 summarizes the common methodology for a PETA analysis and considerations that should be taken into account. Tong (1988) and Rishbeth (2006) posed a series of similar questions regarding data analysis procedures which should be addressed for pre-earthquake anomaly detection. Those questions are equally relevant for PETA and are presented below with modifications where appropriate:

1. What is the nature of the data and its reliability?
2. What is the "normal" behavior of ionospheric TEC in the absence of seismic influences?

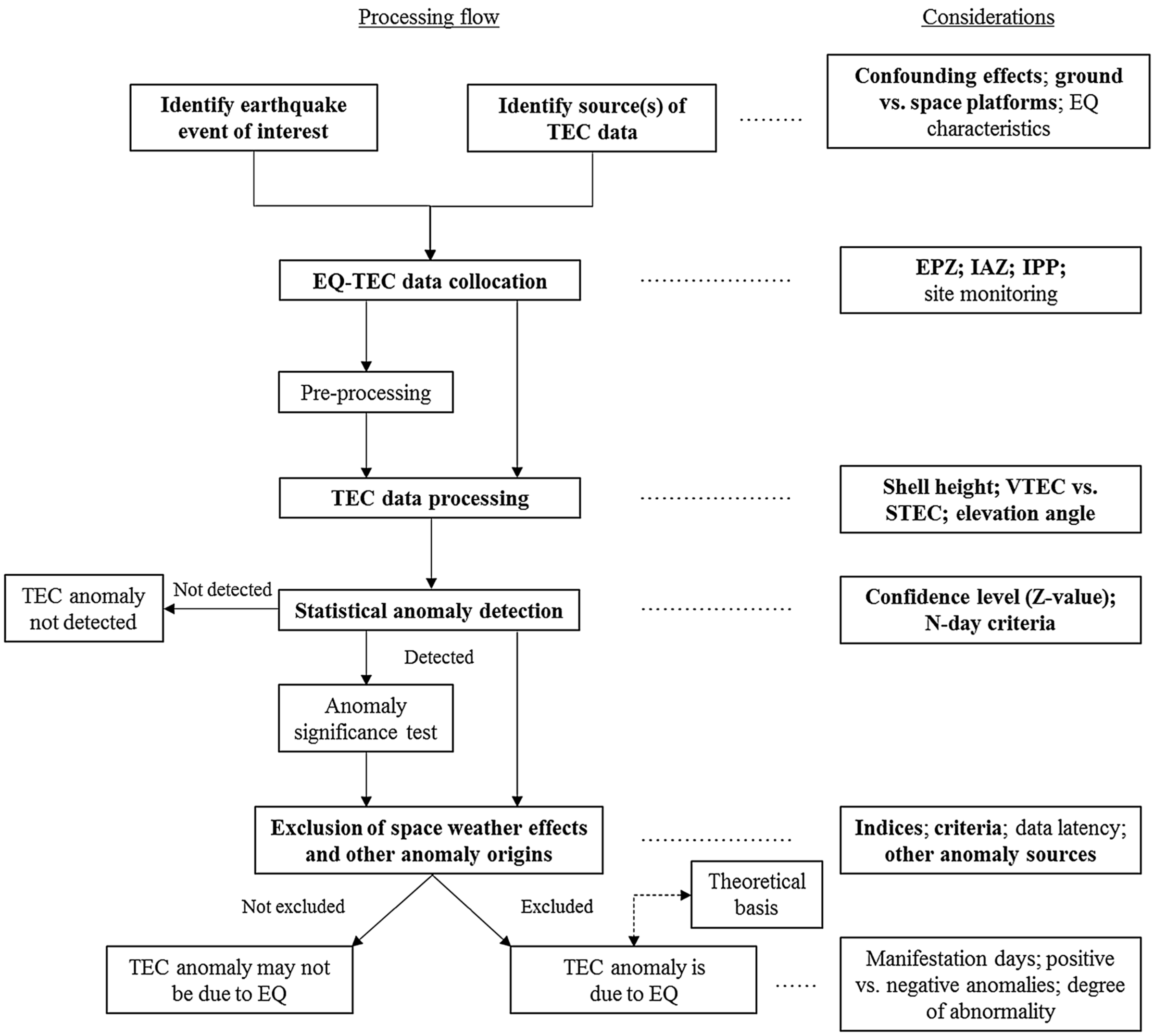


Figure 3
Typical processing for a retrospective (backward-looking) statistical PETA analysis and considerations involved; topics highlighted in bold are addressed in the current study

3. Can a particular geophysical or geochemical change cause the observed ionospheric TEC perturbations?
4. Can non-seismic noise factors be eliminated from the data set?
5. What is the spatial extent of ionospheric TEC that is affected by the pre-earthquake stimuli and what are the limits of detection by ionospheric TEC to different stimuli (e.g. nature of earthquake)?

The above questions are critically examined in the following sections.

### 2.1. *Nature and Reliability of TEC Observations*

Total electron content data can generally be classified based on ground-based or space-borne (i.e. satellite) platforms. The vast majority of retrospective PETA studies have been conducted based on the former, due to the increase in GPS stations over the last decade (Devi et al. 2008; Contadakis et al.

2010). Various GPS networks have been utilized for this purpose. Examples of these are Continuous Operating Reference Station (CORS) (Plotkin 2003), International GNSS Service (IGS) (Hasbi et al. 2009; Lin 2011b; Astafyeva et al. 2014; Aggarwal 2015), Jabatan Ukur dan Pemetaan Malaysia (JUPEM) (Hwa and Zain 2005; Hasbi et al. 2011), Sumatran GPS Array (SuGAr) (Hirooka et al. 2012; Astafyeva et al. 2014), Crustal Movement Observation Network of China (CMONC) (Jin et al. 2015), GPS Earth Observation Network (GEONET) (Astafyeva and Heki 2011; Galvan et al. 2012; Komjathy et al. 2012; Astafyeva et al. 2014), Korean GPS Network (KGN) (Choi and Lee 2016), EUREF Permanent Network (EPN) (Contadakis et al. 2010, 2015), Marmara Continuous GPS Network (MAGNET) (Dogan et al. 2011), Argentine Continuous Satellite Monitoring Network (RAMSAC) (Jiang et al. 2017) and the GPS Ionospheric Scintillation and TEC Monitor (GISTM) (Karia et al. 2013) network. In addition, two-dimensional TEC maps derived from these ground-based observations are also frequently used (Jhuang et al. 2010; Jing et al. 2011; He et al. 2014; Ke et al. 2016). Apart from their convenience and global coverage, ionosphere maps (GIMs), such as those produced using long-term TEC data from the Center for Orbit Determination of Europe (CODE), are regarded as the most precise TEC maps available and typically treated as a high-accuracy reference (Mukhtarov et al. 2013; Wu et al. 2015; She et al. 2017). These ionospheric TEC maps from CODE are generated on an hourly basis and provide relatively good temporal resolution at hourly intervals.

On the other hand, there are comparatively few studies utilizing space-borne TEC data for PETA (Hsiao et al. 2010). This may be due to the lack of satellite platforms carrying relevant instrumentation or performing TEC-related processing (i.e. GPS-derived TEC). In contrast to ground-based GPS stations, satellites provide dynamic observations along their orbit (i.e. location of satellites differs) (Zakharenkova et al. 2016). Compared to ground-based GPS stations, which have typical sampling resolution of 30 s to 2 h, satellites can only measure TEC over a particular location at a lower temporal resolution depending on their orbit characteristics (e.g. polar vs. equatorial revisit rates). As a result, Plotkin (2003) and Galvan et al. (2012) aptly stated that single satellites are often deficient and inadequate for measurement of TEC. However, the recent availability of satellite constellations (e.g. multiple satellites along different orbits) allows for further reductions in sampling time, while simultaneously increasing spatial coverage. Therefore, while ground-based measurements may not provide measurements at locations where earthquakes occur (especially those within oceans where ground stations are unavailable), space-borne systems could overcome such a limitation (Aggarwal 2015). In addition to the FORMOSAT-3/COSMIC-1 satellite, the relatively recent launch of Singapore's climate research satellite VELOX-CI and the satellite constellations SWARM Alpha, Bravo and Charlie by the European Space Agency (ESA) in 2013, along with the follow-up missions of FORMOSAT-7/COSMIC-2 in 2016 and 2018, provide more sources of TEC data for PETA studies, as illustrated in Fig. 4.

To assess the reliability of the two forms of TEC data, a comparison was conducted for a non-seismically active location within Russia (68.6°N 56.9°E) for the year 2016 (Fig. 5), where the closest earthquake ($M_w \geq 4.5$) during that period was located at a distance of approximately 2000 km, in order to examine TEC variations in the absence of earthquake-induced effects. The GIM/CODE TEC (GIM-TEC) was used as reference, while satellite-derived TEC from the SWARM (S3-TEC) and COSMIC (C6-TEC) constellations were acquired. In the conversion of slant (STEC) to vertical TEC (VTEC) and the computation of sub-ionospheric points (SIPs), an ionospheric thin-shell height of 1000 km and elevation angle cut-off of 20° were employed. The thin-shell height was selected to coincide with the altitude of the ionosphere/plasmasphere boundary (thus allowing for maximum probing distance) and to be greater than the satellites' orbital altitudes (Carpenter 2004; Mazzella 2009; Karatay et al. 2010; Dieminger et al. 2012). The direct comparison of ground- and satellite-based TEC is not a straightforward process, since the multiple GPS links in the case of satellites would cause noisy TEC measurements (Zakharenkova et al. 2016). To address this concern, the seasonal variability of VTEC, which is characterized

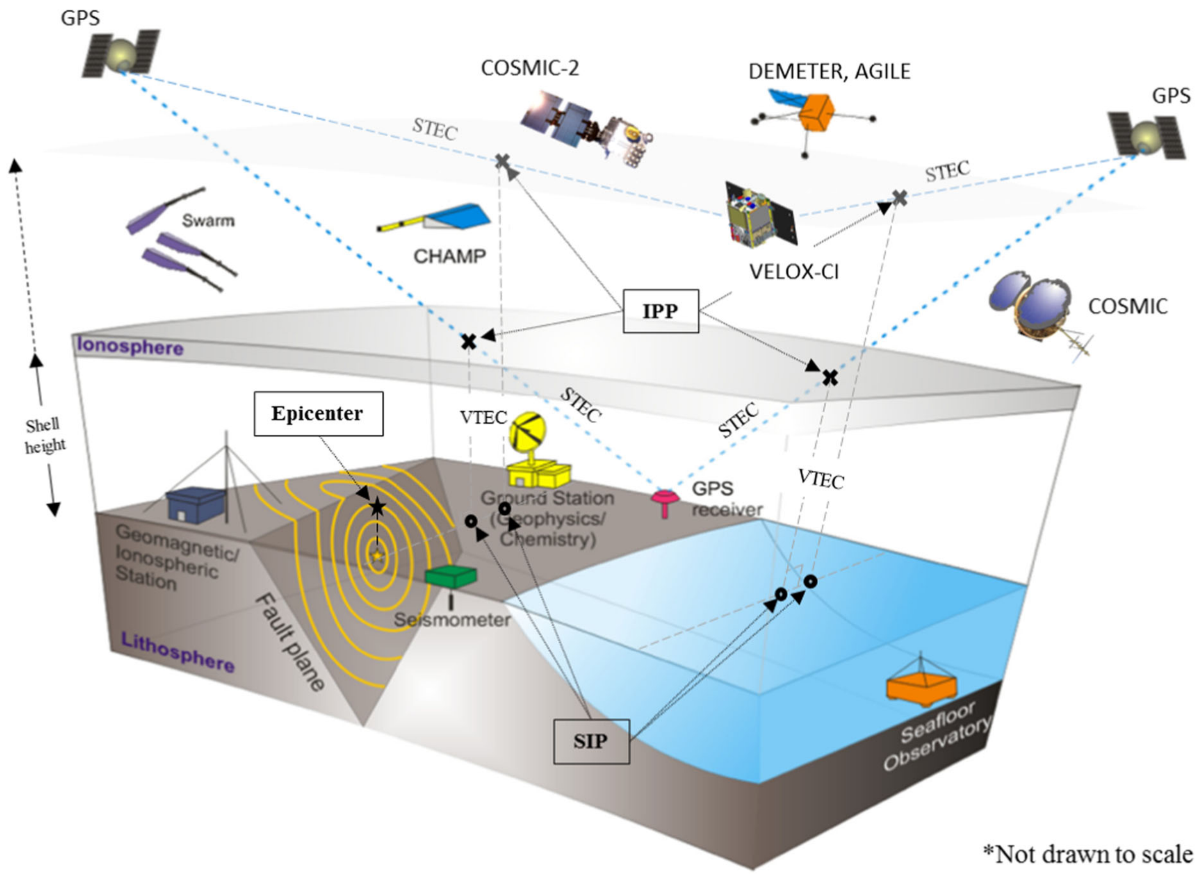


Figure 4
Integration of ground-based and space-borne assets for monitoring of PETA and associated effects [adapted from Tsai et al. (2004) and De Santis et al. (2015)]

primarily by semi-annual and annual components, along with weaker transient patterns, is considered (Mukhtarov et al. 2013; Natali and Meza 2011). Thus, for a coherent comparison, the background VTEC values were extracted using a Savitzky–Golay filter to account for semi-annual variability, which preserves low-frequency TEC structures (Savitzky and Golay 1964).

The VTEC time series are shown in Fig. 6, where several observations can be made. Firstly, the overall TEC variations for each platform are similar, where the symmetrical semi-annual behavior is seen from the VTEC peaks between the months of April and July 2016. The differences between satellite-based and ground-based TEC values were also most pronounced within this period. Secondly, ground-based TEC values registered the highest values as compared to satellite-based TEC across the year. This is expected, as the GPS signals traverse a longer path to reach the ground receivers than satellite receivers, consequently yielding larger STEC values. Thirdly, S3-TEC trend better reflects the semi-annual pattern exhibited by GIM-TEC, whereas C6-TEC variation was relatively flat. The reasons for these occurrences are that (1) SWARM's orbit (approximately 500 km) is at a lower altitude than COSMIC (approximately 800 km), which allows a longer signal path for the dual GPS frequencies, and (2) since the electron density in the plasmasphere (above 1000 km altitude) is significantly less than the contributions in the ionosphere, SWARM's TEC would have probed the more "electron-rich" part of the ionosphere (Wu et al. 2015). This is further reflected by a strong cross-correlation between daily-averaged GIM-TEC

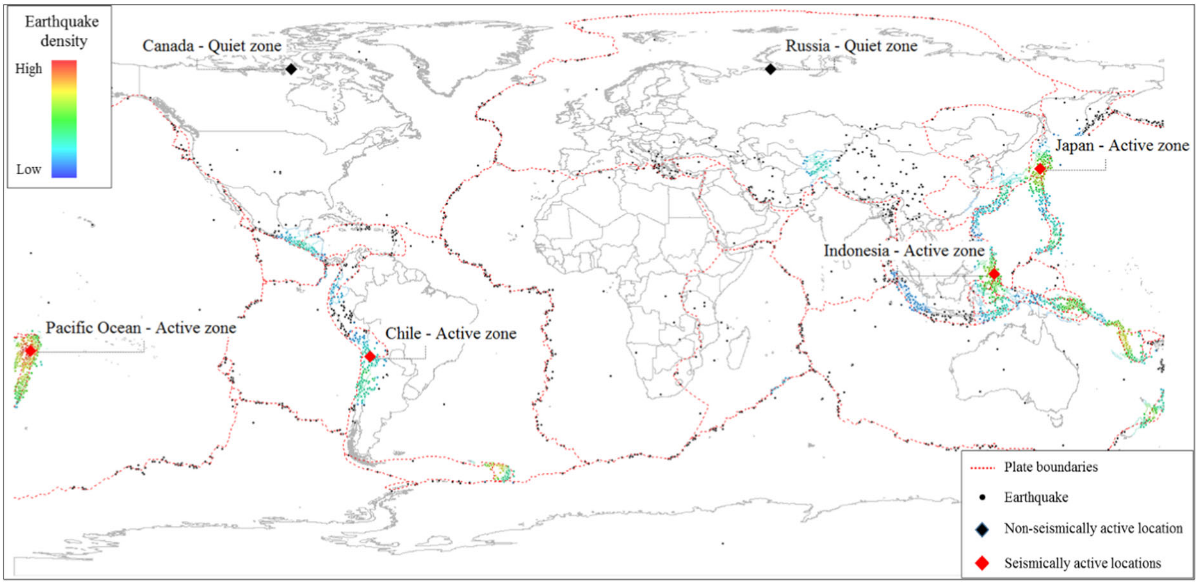


Figure 5
Seismically active (densest earthquake clusters) and non-seismically active (quiet) zones

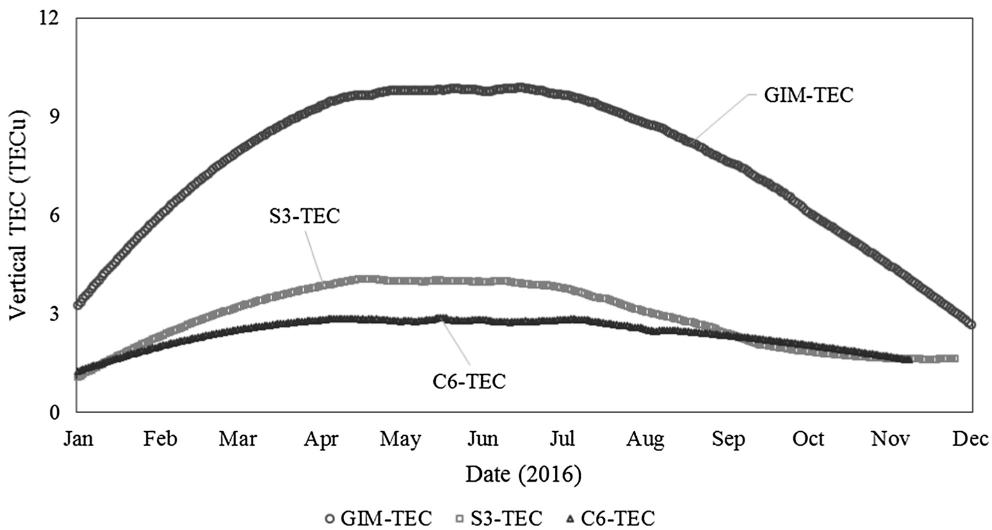


Figure 6
Background VTEC from three TEC sources over a non-seismically active location in Russia (68.6°N 56.9°E) for year 2016

and S3-TEC values, with a correlation coefficient of 0.86 against 0.40 for the case of C6-TEC. Therefore, if TEC data are required over land, GIM-TEC is the ideal choice. However, if the location of interest is over the ocean where ground-based GPS stations are poorly distributed or if intra-hour measurements are needed to improve temporal resolution, both S3-TEC and C6-TEC would act as a potential synergistic supplement to GIM-TEC, although the former is preferred (Ping et al. 2004).

Table 1

*Long-term (annual) VTEC standard deviations for seismically non-active and active zones*

| Year | Zones | | | | | |
|---|---|---|---|---|---|---|
| | Non-active | | Active | | | |
| | Canada 68.6° N 93.4° W | Russia 68.6° N 56.9° E | Chile 21.5° S 68.7° W | Japan 37.3° N 141.4° E | Indonesia 4.3° N 126.9° E | Pacific Ocean 19.8° S 175.1° W |
| 2015 | 6.21 (5.10) | 7.13 (5.66) | 20.7 (19.1) | 9.12 (7.83) | 19.8 (19.0) | 16.7 (14.0) |
| 2016 | 3.77 (3.08) | 3.96 (2.98) | 14.3 (13.3) | 5.04 (4.40) | 13.6 (13.2) | 11.5 (9.71) |

Values in parentheses refer to standard deviations for detrended VTEC

### 2.2. *Seismically Active vs. Non-Seismically Active Zones*

The fundamental objective (i.e. alternative hypothesis) of a retrospective PETA analysis is to establish that ionospheric TEC perturbations are due to a specific earthquake. Thus, the influence of spatially and temporally adjacent earthquakes must be considered. In seismically active regions (especially for countries situated along tectonic plate boundaries), such effects are even more pronounced, as earthquakes are not only clustered together, but occur within days (or even hours) of one another. For example, in the highly seismically affected areas of Japan and South America (primarily Chile) for the year 2016, the average temporal gaps between adjacent $M_w \geq 4.5$ earthquakes were 0.81 and 0.62 days, respectively. Assuming that all earthquakes contribute to TEC changes, the ionosphere above these locations would likely be in a constantly perturbed state. To illustrate this behavior, the statistical dispersions for VTEC (GIM/CODE) in several seismically active and non-seismically active (or quiet) zones (Fig. 5) were examined using two years of data (2015 and 2016). The analyses consisted of both long-term (annual) and short-term (15- and 30-day) VTEC standard deviations. The seismically active zones were identified on the basis of a global inventory of earthquakes ($M_w \geq 4.5$) from the United States Geological Survey (USGS), where the densest earthquake clusters were derived from a kernel density analysis. These regions include Chile, Japan, Indonesia and within the Pacific Ocean, while the selected non-seismically active regions are located in Canada and Russia.

Table 1 summarizes the long-term annual VTEC standard deviations for these regions. The standard deviations for non-seismically active regions were consistently lower than those for seismically active regions for both raw and detrended VTEC values. Among the four seismically active regions, Chile exhibited the greatest variability, where the annual standard deviation was greater than three times (3.8 for year 2016) that of the non-seismically active region (Canada). Japan VTEC readings showed the least dispersion among the seismically active regions, where its standard deviation was approximately up to an average of 1.4 times that of the non-seismically active region in 2015 and 2016. Table 2 shows the results for the short term. The short-term VTEC variations in seismically active regions compared to non-seismically active regions are observed to be greater than the annual variations. For the case of Chile in 2016, the 15-day standard deviation was more than four times that of Canada and Russia. However, Indonesia demonstrated even larger VTEC variation with its complex geology, as several tectonic plates converge at its location. The 15-day standard deviation ratio (year 2016) for Indonesia compared to Russia were as high as 4.5, while for daily-averaged detrended VTEC values, the ratio was close to 2 (Fig. 7). In summary, three observations can be deduced: (1) seismically active regions exhibit greater TEC variability than non-seismically active regions; (2) short-term variations are stronger than their long-term annual counterpart, which can be attributed to the temporally localized earthquake preparatory effects on the ionosphere; and (3) smaller earthquakes (not necessarily only large-magnitude

Table 2

*Short-term (15- and 30-day) moving average VTEC standard deviations for seismically quiet and active zones*

| Year | Zones | | | | | |
|---|---|---|---|---|---|---|
| | Quiet | | Active | | | |
| | Canada<br>68.6° N<br>93.4° W | Russia<br>68.6° N<br>56.9° E | Chile<br>21.5° S<br>68.7° W | Japan<br>37.3° N<br>141.4° E | Indonesia<br>4.3° N<br>126.9° E | Pacific Ocean<br>19.8° S<br>175.1° W |
| 2015 | 4.34 (7.60) | 4.66 (8.34) | 16.0 (25.4) | 6.35 (10.9) | 16.9 (24.7) | 11.8 (20.3) |
| | 4.25 (7.01) | 4.65 (7.95) | 15.6 (25.1) | 6.27 (10.7) | 16.5 (24.5) | 11.4 (19.6) |
| 2016 | 2.82 (4.96) | 2.65 (5.38) | 11.4 (17.3) | 4.03 (6.69) | 12.0 (16.7) | 8.11 (16.6) |
| | 2.75 (4.92) | 2.63 (5.04) | 11.0 (17.1) | 3.95 (6.59) | 11.6 (15.9) | 7.75 (16.4) |

Top row refers to 15-day values, while bottom row refers to 30-day values

Values in parentheses refer to maximum standard deviation values

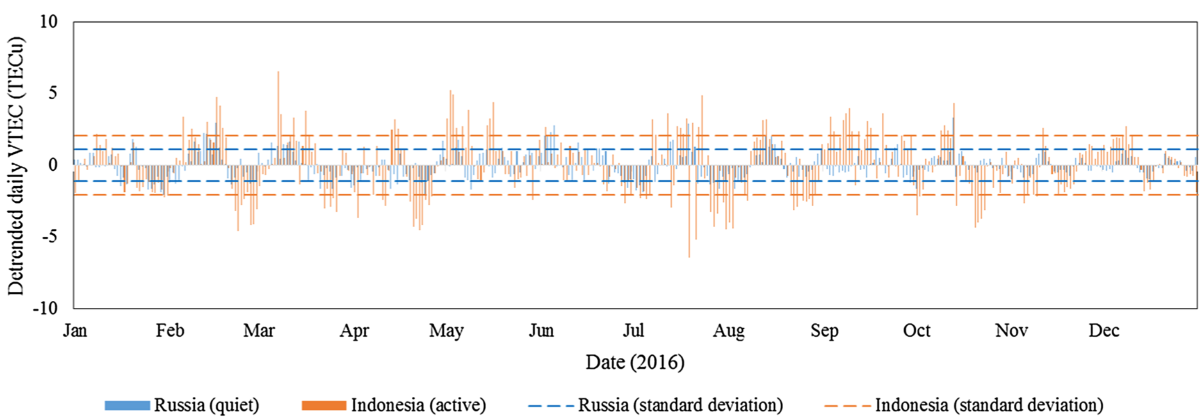


Figure 7
Daily-averaged and detrended GIM-TEC values for Russia and Indonesia for the year 2016

main shock events) can induce ionospheric perturbations as well. Consequently, for a retrospective PETA analysis, it is necessary to ascertain the state of ionospheric variability (i.e. determining whether or not the location is in a seismically active region) and adjust anomaly detection methods accordingly to prevent false positives or negatives (Guo et al. 2016). For example, in areas of high seismic activity, the standard deviations used in the statistical envelope method might be too high, leading to false-negative cases. Simply testing for the existence of PETA with regard to a large-magnitude earthquake within an earthquake swarm (which is typically the case for large seismic events) could be problematic due to influence of adjacent earthquakes and the recurrence times of earthquakes (Liu et al. 2010a). The simultaneous exclusion of these two effects were addressed by Le et al. (2011), where a period of 15 days before and after were excluded if an adjacent earthquake occurred within a 5° zone. Nonetheless, studies accounting for adjacent earthquake effects are rare.

### 2.3. *Anomaly Detection by Statistical Envelope Methods*

Depending on the nature of the TEC data used, there are several techniques to determine whether a particular TEC data point is anomalous. For example, in the case where two-dimensional TEC maps are used, novel algorithms involving parametric (i.e.

pattern recognition) analyses (e.g. neural network, wavelet transform, support vector machine) have recently been explored (Akhoondzadeh 2013c, d, 2015; Sompotan et al. 2015). While the general conclusion of these analyses indicated the existence of PETA owing to a particular earthquake, such analyses require more justification in the definition of background TEC behavior. Furthermore, other techniques such as the cubic fit analysis method adopted by Heki (2011) was shown to yield erroneous interpretations of anomalies (Kamogawa and Kakinami 2013; Masci et al. 2015).

Since earthquakes are statistical in nature (e.g. Gutenberg–Richter law), statistics-based approaches have also been used in the detection of PETA (Chen et al. 2004; De Santis et al. 2015). These approaches include relative deviation (Kouris and Fotiadis 2002; Kouris et al. 2006), time derivative analysis (Ciraolo and Spalla 1999), correlation analysis (Leyva-Contreras et al. 2005; Pulinets et al. 2007), TEC difference analysis (Plotkin 2003) and ionospheric correction (Trigunait et al. 2004). In addition to the statistics-based approaches, statistical envelope methods (e.g. *N*-day moving mean- and median-based techniques) for the detection of PETA are becoming more common and have become popular (Astafyeva and Heki 2011; He et al. 2012; Pundhir et al. 2014; Dai et al. 2015). Additionally, several researchers have previously emphasized that the detection of pre-seismic TEC anomalies should be based on a statistical time-series investigation (Liu et al. 2004; Guo et al. 2015; Masci et al. 2015).

In the mean statistical envelope method, the TEC of a particular point in time ($\mathrm{TEC_{CURRENT}}$) is compared against the previous *N*-day mean TEC values ($\mathrm{TEC_{MEAN,N}}$), with upper and lower bound constructed using the associated standard deviation ($s$). An anomaly therefore occurs when $\mathrm{TEC_{CURRENT}}$ exceeds the bounds defined by $Z$ and $s$ (Eq. 1). Equation (2), which is similar in form to Eq. (1), is applied in the median method (Liu et al. 2010a; Dogan et al. 2011; Ulukavak and Yalcinkaya 2016) on the basis of upper (UQ) and lower (LQ) quartiles (typically with $k = 1.5$). Under the assumption of normal distribution, UQ and LQ could in fact be approximated by $Zs$ (with $Z = 1.34$) (Klotz and Johnson 1983; Aggarwal 2015):

$$\mathrm{PETA} : |\mathrm{TEC_{CURRENT}}| > \mathrm{TEC}_{\mathrm{MEAN},N} + Zs, \qquad (1)$$

$$\mathrm{PETA} = \begin{cases} \mathrm{TEC_{CURRENT}} > \mathrm{TEC}_{\mathrm{MEAN},N} + k\left(\mathrm{UQ} - \mathrm{TEC}_{\mathrm{MEAN},N}\right) \\ \qquad\qquad or \\ \mathrm{TEC_{CURRENT}} > \mathrm{TEC}_{\mathrm{MEAN},N} - k\left(\mathrm{TEC}_{\mathrm{MEAN},N}z - \mathrm{LQ}\right) \end{cases}. \qquad (2)$$

As such, there are two major parameters when using the statistical envelope method: *N*-day and *Z*. *N*-day refers to the number of days before the earthquake event used for anomaly detection. Ideally, *N*-day should be as large as possible to provide better statistical characterization and yet small enough to capture local variability (Karatay et al. 2010). There is a need to prescribe *N*-day corresponding to systematic background TEC fluctuations such as the diurnal TEC variability caused by sunrise and sunset (i.e. magnetic local times) (Nenovski et al. 2015). However, currently there is no clear justification for the selection of *N*-day used in previous PETA studies, for example, *N*-day = 5 (Nenovski et al. 2015), 10 (Yiyan et al. 2009; Xu et al. 2013), 15 (Chen et al. 2004; Chauhan et al. 2009; Liu et al. 2010a; Hirooka et al. 2012; He et al. 2014; Aggarwal 2015; Ke et al. 2016; Ulukavak and Yalcinkaya 2016; Thomas et al. 2017), 27 (Guo et al. 2015), 30 (Jhuang et al. 2010; Guo et al. 2016) or 60 (Xu et al. 2013). Consequently, statistical envelope methods face the challenging task of accounting for ionospheric variability (owing to different phenomena such as space weather and possible seismic effects) within a single *N*-day.

Currently, the influence of *N*-day on the number of days leading up to the earthquake event ($n_{\mathrm{pre}}$) is not adequately quantified (i.e. approximation of the time of earthquake, should an anomaly be detected). For example, Karatay et al. (2010) defined a 30-day earthquake-day period (EDP) consisting of 15 days before and after an earthquake, when the ionosphere is presumed to be under a state of seismic-induced perturbation. Thus, PETA detected within a 15-day window would suggest the likelihood of an earthquake occurring within 15 days. Plotkin (2003) reported $n_{\mathrm{pre}}$ of 2 days for an $M_{\mathrm{w}}$ 6.6 event, while Liu and Xu (2017) and Chauhan et al. (2009) reported $n_{\mathrm{pre}}$ of 0–6 days for $M_{\mathrm{w}}$ 7.0 and $M_{\mathrm{w}}$ 4.5–5.1 earthquakes, respectively. Singh et al. (2009)

concluded that for 43 events of $M_w \geq 5$ (average magnitude = 5.6), $n_{pre}$ was between 0 and 9 days, and similarly, Yiyan et al. (2009) found $n_{pre}$ to be up to 9 days. More recently, Guo et al. (2015) established that $n_{pre}$ could be as long as 11 days from two events which occurred in 2012 ($M_w$ 8.6 in Sumatra and $M_w$ 6.7 in Mexico). Figure 8 depicts the frequency of $n_{pre}$ (based on statistical envelope methods) from the literature and shows that $n_{pre}$ may be up to 2 weeks before an earthquake, while $n_{pre}$ = 3 days has been most frequently observed. Figure 9 illustrates the variations in average $n_{pre}$ with earthquake magnitude, where $n_{pre}$ exhibited greater variability at larger earthquake magnitudes, with the exception of $M_w \geq 9.0$ (perhaps due to fewer occurrences of such events). These results thus show that large-magnitude earthquakes exhibit greater variability regarding the manifestation time of PETA.

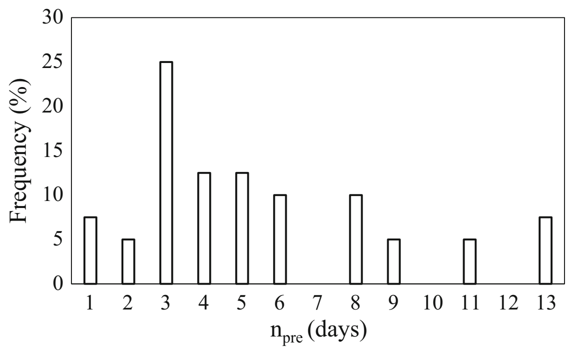


Figure 8
Frequency of $n_{pre}$ reported in the literature for statistical envelope methods

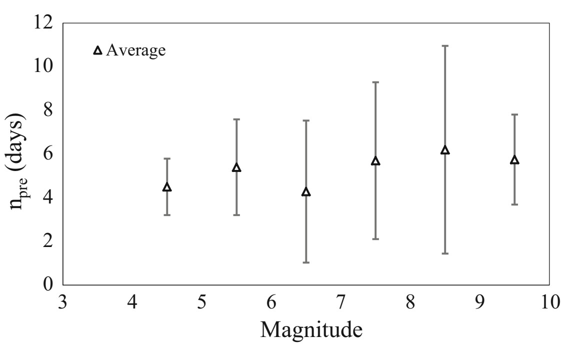


Figure 9
Variations in average $n_{pre}$ and associated standard deviations with earthquake magnitude for statistical envelope methods

Nonetheless, neither Figs. 8 nor 9 differentiates between finer details such as earthquake nature or sign of PETA anomaly (i.e. positive vs. negative).

Equations (1) and (2) show that the detection of PETA based on statistical envelope methods is associated with a confidence level (i.e. $Z$) which defines the envelope of normal ionospheric variations. Previous studies have suggested values of $Z$ = 1 (Karatay et al. 2010; Contadakis et al. 2015), 1.34 (Hasbi et al. 2011; Nenovski et al. 2015), 1.5 (Liu et al. 2010a; Akhoondzadeh 2013b), 1.96 (Dogan et al. 2011), 2 (Molchanov and Hayakawa 1998; Chauhan et al. 2009; Jhuang et al. 2010; Jing et al. 2011; Contadakis et al. 2015), 2.5 (Jhuang et al. 2010), 2.9 (Jhuang et al. 2010) and 3 (Contadakis et al. 2015; Thomas et al. 2017). Figure 10 shows the variations in $Z$ with confidence levels (according to probability theory) plotted over the ranges of $Z$ used in the literature. $Z$ governs the detection of PETA and is critical for distinguishing false positives (Chen et al. 2004). $Z$ has been related to earthquake magnitude (Krankowski et al. 2006; Yiyan et al. 2009; Kon et al. 2011). Large-magnitude earthquakes tend to induce a greater degree of PETA (Perevalova et al. 2014, Jin et al. 2015; Šlégr and Váňová 2017). These results consequently imply that smaller-magnitude earthquakes could only be detected with lower $Z$, since the effect on the ionosphere due to these earthquakes would similarly be lower (Lin 2011a). Recently, Ke et al. (2016) and Guo et al. (2015) challenged this notion and concluded that a greater degree of PETA was not observed in larger-magnitude earthquakes. Since the prescription of $Z$ restricts the magnitude of earthquakes (i.e. lower bound) that

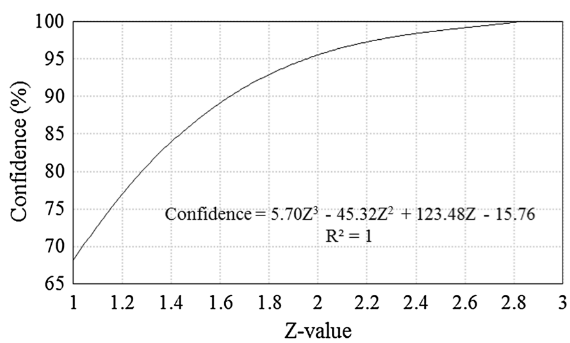


Figure 10
Variation of $Z$-values with confidence levels

can be detected, more work is needed to ascertain the appropriate $Z$-value for use in statistical envelope methods.

### 2.4. Exclusion of Space Weather Effects and Other Sources of Ionospheric TEC Perturbations

In order to attribute earthquake as the sole cause of ionospheric perturbation, other sources (e.g. space weather effects such as solar flares, magnetic storms) which may affect ionospheric TEC must be excluded (Liu et al. 2006b; Zhu et al. 2018). Such checks are made when PETA is detected to exclude space weather effects using geomagnetic indices such as Kp, disturbance storm time (Dst) and solar flux index F10.7 (Saba et al. 1997; Devi et al. 2014). As mentioned earlier, the straightforward use of these indices is problematic, and made worse by the highly variable state of the ionosphere before and after an earthquake (Heki and Enomoto 2013; He et al. 2014). For instance, Kon et al. (2011) showed that positive PETA was induced by 52 $M_w \geq 6$ earthquakes in Japan. However, their study may have misinterpreted the normal levels of geomagnetic activity (Masci 2012).

Figure 11 presents the variations in the number of space-related indices used to exclude space weather effects from a sample of 50 PETA case studies in the literature. Figure 11 shows that verifications relying on either one or two indices were the most common. The frequency of various space weather indices [i.e. geomagnetic—Kp, Dst, Ap, AE, solar-related—F10.7, EUV, SSN, interplanetary fields—Bz

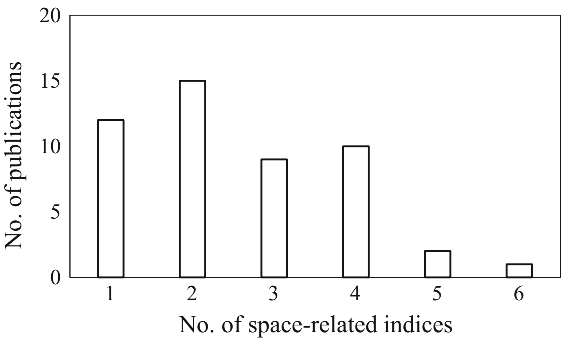


Figure 11
Number of space-related indices used in the literature

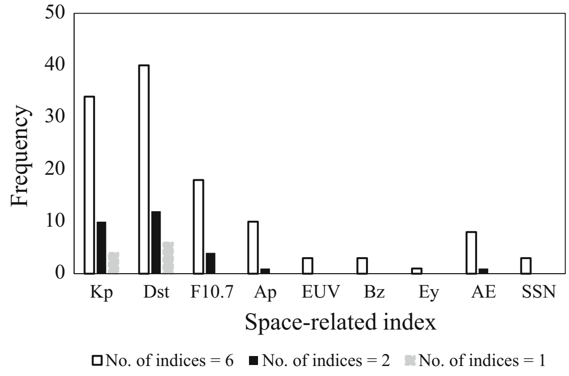


Figure 12
Frequency of individual space-related index used in the literature

(magnetic), Ey (electric)] in relation to the number of different indices (i.e. total of one, two or six indices for each case study) being cited is further highlighted in Fig. 12. A closer examination of the specific indices in Fig. 12 reveals that the most frequently used indices were Dst, Kp and F10.7, in that order. At present, there is no consensus on the values of the indices. For example, acceptable (i.e. either quiet or low) geomagnetic activity may be identified on the basis of Kp with a value less than 2 (Klimenko et al. 2011), 2.5 (Hayakawa and Molchanov 2002; Liu et al. 2004; Pulinets and Boyarchuk 2004), 3 (Chauhan et al. 2009; Singh et al. 2009), 4 (Hasbi et al. 2011), 5 (Dogan et al. 2011) or 6 (Karatay et al. 2010). Karia et al. (2012) used cumulative values of Kp below 20 over 8 days, and Ke et al. (2016) used Kp values below 30 within 1 day. When the parameter of Dst (units of nanotesla) is used to indicate geomagnetic levels, threshold values of 10 (Klimenko et al. 2011), 15 (Hasbi et al. 2011), 20 (Liu et al. 2004; Pulinets and Boyarchuk 2004; Dogan et al. 2011), 40 (Jiang et al. 2017), 50 (Ke et al. 2016) and 60 (Kon et al. 2011) have been used. To account for solar-related effects, the F10.7 index was used as a proxy for the solar extreme ultraviolet (EUV) flux, which ionizes the neutral atmosphere in the ionosphere (Liu et al. 2011; Bruevich and Yakunina 2014). Similar to Kp and Dst, many values of F10.7 have been used to indicate low solar activity levels. Values of F10.7 (solar flux units) lower than 70 (Guo et al. 2015), 100 (Akhoondzadeh 2013d), 120 (Hayakawa and Molchanov 2002; Liu et al. 2004; Pulinets and Boyarchuk

2004), 130 (Akhoondzadeh 2013a) and 150 (Jiang et al. 2017) have been used.

The choice of suitable indices could be justified based on location, depending on data availability and station coverage (e.g. Dst for equatorial regions, and Kp for global/polar latitudes) (Jhuang et al. 2010). However, the values of these indices used for defining space weather activity levels (e.g. quiet, low, moderate, high) may eventually lead to incorrect identification of PETA, resulting in both false-positive and false-negative cases. Ideally, all relevant space weather indices should be verified for quiet or low activity levels in order to confidently demonstrate the lack of space-related influences on ionospheric perturbations. As some of the indices are not independent, a judicious selection could reduce the number of indices considered. For example, the geomagnetic indices of Kp and Ap differ in terms of scale used (Saba et al. 1997), where Kp is represented on a quasi-log scale, Ap is based on the linear scale, and the choice of either one may suffice. To circumvent the subjectivity of activity levels, statistics-based methods could be applied on space weather indices. For example, Jhuang et al. (2010) employed standard deviations (similar to the PETA detection process) to objectively analyze the significance of space weather variations. The use of such procedures could provide better justification of the values of the space weather indices. However, there is no consensus on the procedures.

Furthermore, the likelihood remains that TEC anomalies may be due to sources other than space weather or seismic preparation effects (Komjathy et al. 2012). For example, geophysical processes such as volcanic eruptions (Lin 2013) and tsunamis (Galvan et al. 2012), and man-made events such as nuclear tests (Kakinami et al. 2011), rocket/missile launches (Ding et al. 2014; Kakinami et al. 2013) and even scientific experiments such as the High Frequency Active Auroral Research Program (HAARP), have been shown to cause ionospheric perturbations (Karia et al. 2012). The simultaneous occurrence of these processes with seismic preparation effects is likely to be rare compared with space weather phenomena. Nonetheless, possibilities for non-seismic-related TEC anomalies must be accounted for when detecting PETA.

### 2.5. *Extent of Ionospheric Perturbations*

To spatially associate TEC measurements (whether from ground- or space-based platforms) to a particular earthquake, TEC samples falling within the "earthquake preparation zone" (EPZ) are conventionally assumed to be spatially collocated (i.e. attributed to that earthquake). Based on studies such as Liu et al. (2001), Pulinets et al. (2003), He et al. (2014) and Guo et al. (2015), PETA is most significant at a distance from the epicenter. The EPZ may not be circular with the center at the epicentre (Bowman et al. 1998). However, most retrospective case studies determine PETA at the epicenter (Liu and Xu 2017). Various EPZ equations have been proposed. The most frequently used equation was that suggested by Dobrovolsky et al. (1979), as follows:

$$R = 10^{0.43 M_w}, \quad (3)$$

where $R$ is the radius (km) and $M_w$ is the earthquake magnitude. According to Eq. (3), large-magnitude earthquake events (e.g. $M_w$ 7.0 and above) typically result in EPZ spanning large areas (e.g. EPZ radius for an $M_w = 7.0$ earthquake is approximately 1023 km). The usefulness of the exponential scaling relationship given by Eq. (3) for approximating an earthquake's location is limited, since the dimensions of EPZ can theoretically cover one third of the earth's surface for an $M_w$ 9.0 earthquake (i.e. radius larger than 7000 km) (Masci and Thomas 2015; Thomas et al. 2017). Other equations (e.g. Kondratenko and Nersesov 1962; Anderson and Whitcomb 1975;

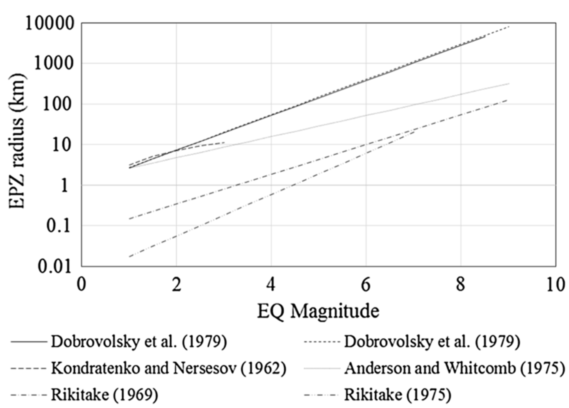


Figure 13
EPZ radius dependence on earthquake magnitude reported in the literature

Rikitake 1969, 1975) for estimating the EPZ are illustrated in Fig. 13. Figure 13 shows that the EPZ determined from Dobrovolsky et al. (1979) differs from Rikitake (1969) and Rikitake (1975) by two orders or more across the entire range of earthquake magnitudes. The EPZ equations proposed by Rikitake (1969) and Rikitake (1975) were based on anomalous crustal deformations, while the Dobrovolsky et al. (1979) EPZ equation (i.e. Eq. 3) was founded on mostly geochemical precursory phenomena (e.g. radon, helium, carbon dioxide, hydrogen, fluorine and chlorine). It was aptly pointed out that Eq. (3) was not based on experimental evidence, which showed that the actual seismic preparation area is much smaller (Liu et al. 2010a; Masci and Thomas 2014). Comparing pre-seismic crustal deformations (occurring on the earth's surface) and geochemical emanations above the earth's surface (i.e. Eq. 3), the dimensions of the affected area were clearly larger for geochemical emanations, as indicated in Fig. 13. Although the data used in Dobrovolsky et al. (1979) were limited to 24 earthquake events and did not account for ionospheric anomalies, the authors concluded that Eq. (3) could be used to estimate the "effective precursor manifestation zone" (i.e. EPZ), which is independent of the precursor's physical nature. Subsequently, Eq. (3) has been commonly used for investigating PETA (e.g. Chauhan et al. 2009; Liu et al. 2010a, b; Lin 2011b, De Santis et al. 2015; Choi and Lee 2016). In addition, the EPZ radius computed using Eq. 3 is typically prescribed as an upper limit beyond which PETA is assumed not to occur (Devi et al. 2010; Astafyeva and Heki 2011; Akhoondzadeh 2015).

While the use of Eq. (3) is straightforward for collocating TEC data, assumptions made in its formulation may result in erroneous interpretations. Bowman et al. (1998) have provided some justification of Eq. (3) on the basis that the critical region of an earthquake is equal to or less than the thickness of the seismogenic crust. Using data from Benioff (i.e. crustal) strains, Bowman et al. (1998) found such an assumption to be valid only for $M_w \leq 6.0$ earthquakes and suggested that the exponent in Eq. (3) should be increased for $M_w \geq 6.0$ earthquakes, as these earthquakes may rupture the entire crust. In addition, PETA-related studies have yielded conflicting results—while most researchers agree that PETA is most significant within close proximity of the epicenter (i.e. center of EPZ) (e.g. Jiang et al. 2017), other studies have reported that PETA is greatest at the edge of the EPZ (e.g. Liu et al. 2001; Lin 2011b). Šlégr and Váňová (2017) examined the D-layer region of the ionosphere using very low-frequency (VLF) reflected waves and discovered that no ionospheric anomalies were induced by shallow earthquakes beyond the EPZ, thus apparently supporting its validity. However, it should be noted that the altitude of the ionospheric D-layer (approximately below 80 km) is lower than the F-layer (approximately 350–400 km) which is conventionally probed by the TEC technique, and dimensions of the EPZ at F-layer heights would likely be different. Notably, a study involving a large catalogue of strong ($M_w \geq 7.0$) earthquakes conducted by Liu and Xu (2017) revealed that the ionospheric regions which were most perturbed tended to be located south of the epicenter, regardless of the epicenter's geographic position. In this case, Liu and Xu (2017) studied strong earthquakes, and the extent of the EPZ was greater than 1000 km (i.e. $\geq M_w$ 7.0). Consequently, arguments have been put forth where the effects of earthquake preparation on the ionosphere could have a larger radius, and thus any ionospheric perturbations would have been observed even if ground-based stations were located far from the EPZ (Singh et al. 2009; Karia and Pathak 2011). Figure 14 exemplifies the implication of the EPZ if PETA is present within the EPZ, using the distribution of earthquakes along the western section of the Pacific Rim of Fire during the period from 1 January to 31 March 2015. Hence, determining PETA at one location may not mean that the earthquake effects can be felt at that location, given the very large EPZ for a large-magnitude earthquake. Therefore, does the spatial region confined by EPZ truly mark the limits of the PETA affected area?

Hence, while the arbitrary use of EPZ is convenient for spatially identifying the existence of PETA, the EPZ appears to be only a proxy parameter for the actual seismic-induced perturbed region in the ionosphere, and is not properly justified (Masci and Thomas 2015). Here, the term "ionosphere affected zone" (IAZ) is used to refer to this region in the

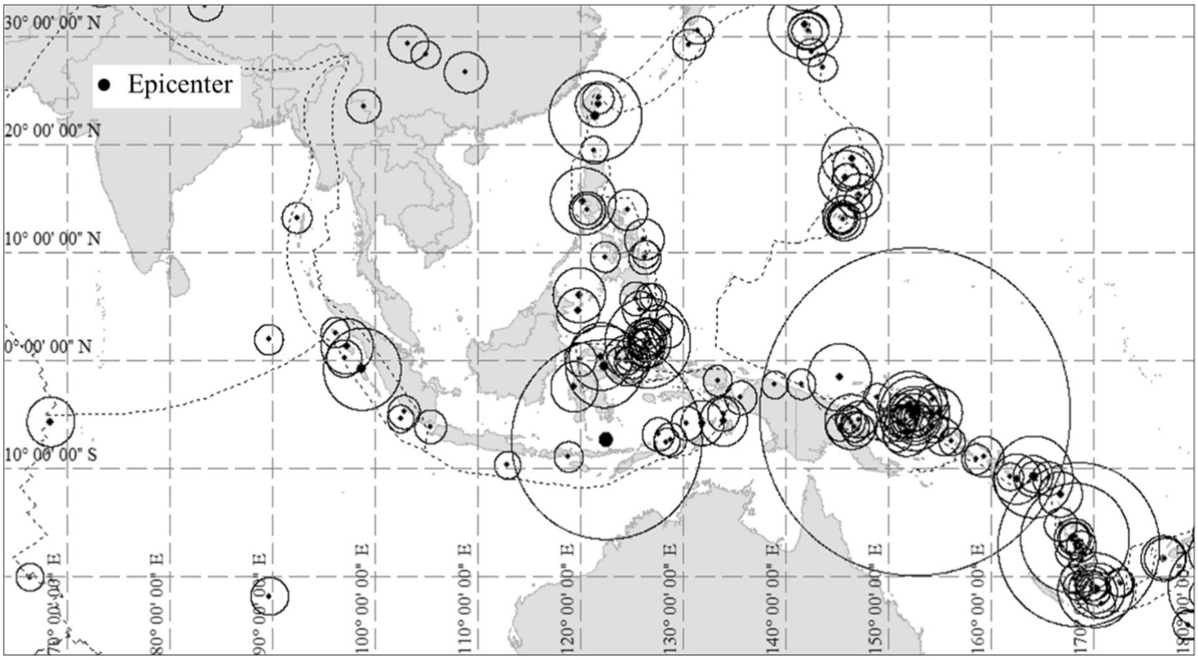


Figure 14
Distribution of $M_w \geq 5.0$ earthquakes (between 1 Jan and 31 Mar 2015) illustrating spatial adjacency effects using EPZ; epicenter symbol is scaled according to magnitude; dashed lines represent tectonic plate boundaries

ionosphere. A schematic of the IAZ with respect to the EPZ and receiver (i.e. LEO and ground station) to GPS links is shown in Fig. 15. Two related parameters are introduced to define the IAZ: $u_{\mathrm{IAZ}}$ essentially accounts for the projection of EPZ onto the ionosphere, while $R_{\mathrm{IAZ}}$ is the radius of the IAZ itself. When EPZ was previously used as a proxy for IAZ, the roles of ionospheric pierce point (IPP) (i.e. latitude, longitude and altitude) and SIP (i.e. latitude and longitude) could be used interchangeably to locate TEC sampling points per receiver–GPS link. However, such a presumption would not be valid with the introduction of IAZ. As mentioned previously, PETA is theoretically detected when TEC samples (i.e. IPP) are within the IAZ. From Fig. 15, the location of IPP within the IAZ does not guarantee the same for SIP within the EPZ.

While the representation of an ionospheric perturbed region by the IAZ is more accurate, its concept is not new. Astafyeva et al. (2013) previously pointed out the possibility of investigating spatial extension of ionospheric perturbations using multiple links from ground-based receivers to GPS satellites. In addition, limited studies have attempted to analyze PETA on the basis of ionospheric tomography, with interesting results. For example using two-dimensional principal component analysis (PCA), Lin (2011b) discovered that while anomaly intensity increases, the spatial distribution of PETA decreases with increasing altitude, thereby implying that $u_{\mathrm{IAZ}}$ is greater than 90° (i.e. if $u_{\mathrm{IAZ}} = 90°$, IAZ = EPZ), while Dobrovolsky et al. (1979) stated that the size of the IAZ is of the same order as the EPZ. If $R_{\mathrm{EPZ}} < R_{\mathrm{IAZ}}$, the EPZ becomes a more stringent parameter set for the detection of PETA. The establishment of IAZ provides greater insight into PETA spatial manifestations and increases the likelihood of its detection due to the availability of more collocated data.

A possible complication in earthquake forewarning stemming from the use of IAZ (or EPZ), apart from its exponential scaling relationship, is the epicenter's ambiguity problem arising from TEC observables of a satellite-based GPS receiver. Since the epicenter location of an earthquake is known for retrospective analyses, a single IAZ defines the zone

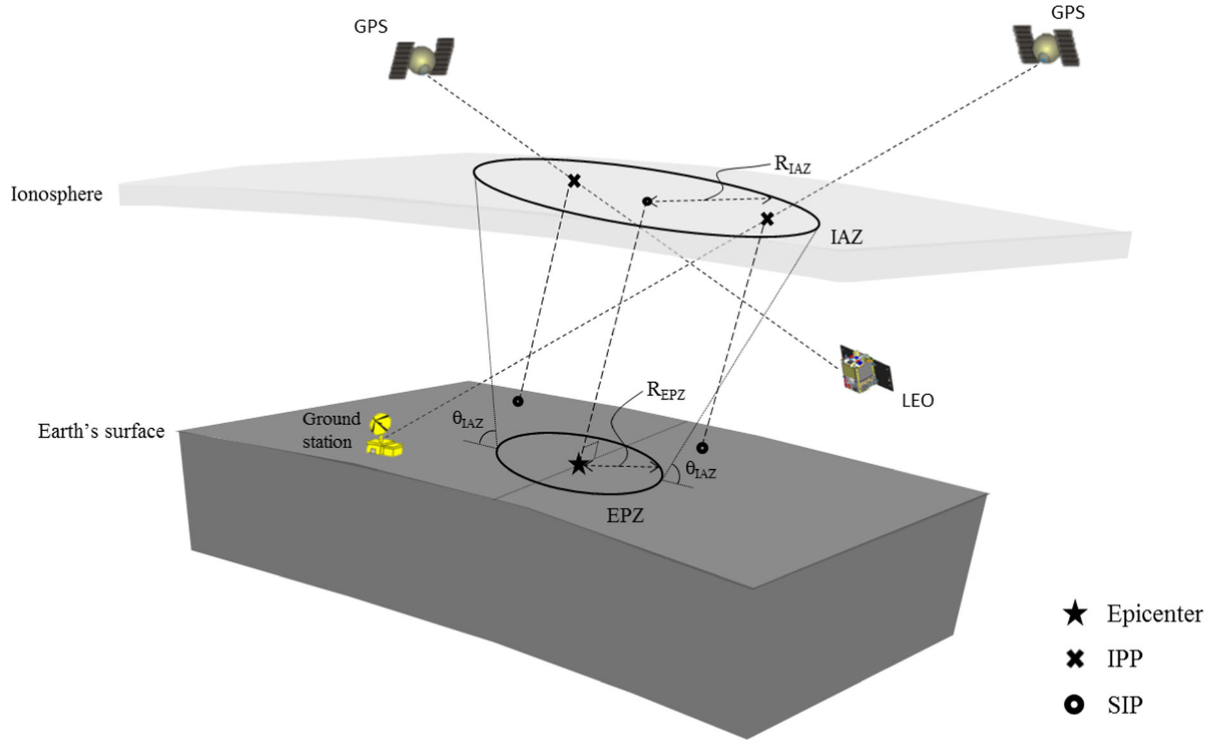


Figure 15
Illustration of ionosphere affected zone (IAZ) in relation to EPZ

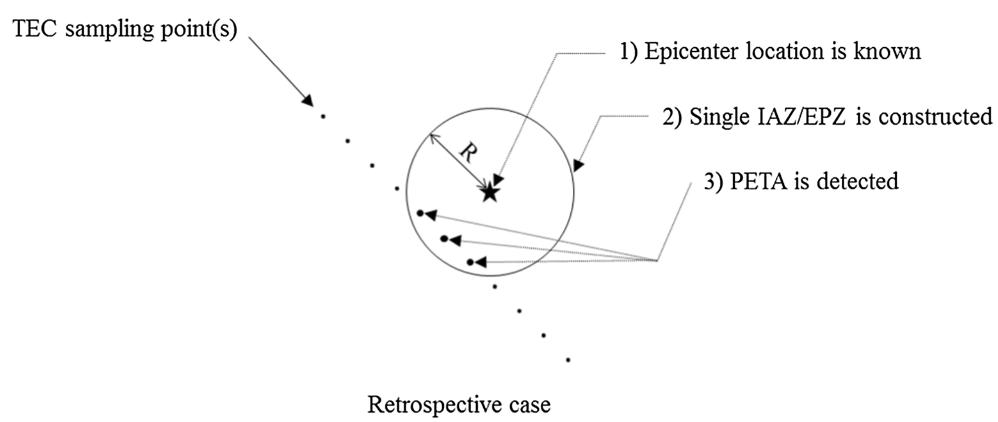


Figure 16
Absence of epicenter ambiguity (retrospective case)

for which PETA is detected (Fig. 16). The converse, however, is not true. In prospective analyses, the detection of a single PETA point allows more than one IAZ to be constructed provided that anomalous TEC data fall within these zones. Consequently, the potential earthquake epicenter could lie anywhere within the IAZs. For the theoretical unbounded case (Fig. 17), the epicenter could be located anywhere within a circular zone of radius 2R from the detected anomaly. This thus poses a significant

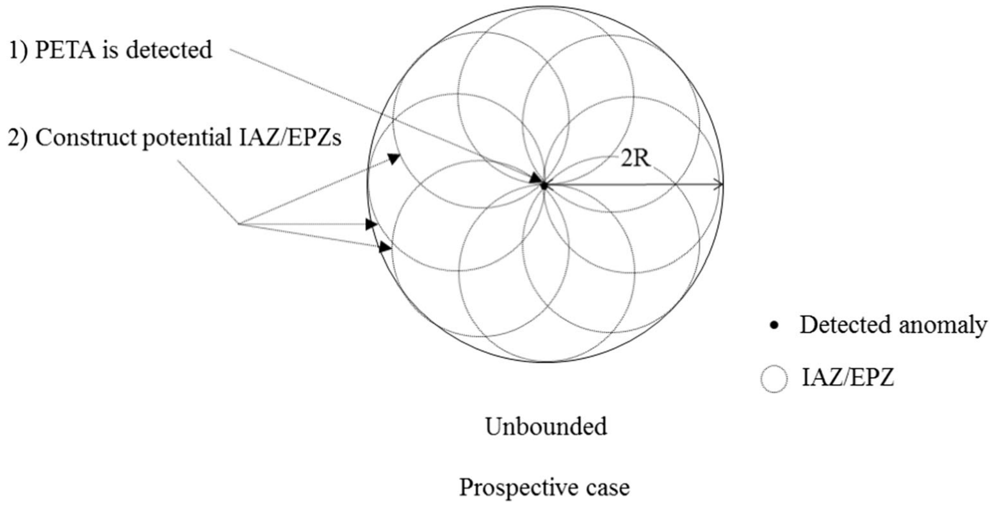


Figure 17
Unbounded epicenter ambiguity (prospective case)

challenge in ascertaining the location of the seismic event in the absence of supplementary information (e.g. plate boundaries, potential fault zones, and correlations involving degree of PETA and epicentral distance).

### 3. The Future of PETA

As many TEC sources are increasingly made available in the coming decade, due considerations regarding their differences must be addressed. Several points with regard to the inherent differences between ground and space data sources and TEC processing methodologies (i.e. shell height, STEC vs. VTEC, elevation angle) in the literature were highlighted. These pertain to the nature of the data and potential errors arising from differing assumptions made in processing the parameters. These inconsistencies potentially hinder the application and integration of past experiences and results for the establishment of an earthquake forewarning system using PETA. The availability and temporal resolution of ground-based TEC measurements act as a constant source of measurements. Satellite-derived TEC, on the other hand, may or may not provide timely data (depending on whether constellations are used), but they are valuable for understanding the dynamic characteristics of PETA with respect to the epicenter, without the need for interpolation (as with two-dimensional TEC maps). As mentioned by Lin (2011b), knowledge of PETA spatial distributions is important, as it could point towards the origin of seismic activity. Therefore, the degree of PETA (i.e. how anomalous it is compared with normal variations) in relation to epicentral distance and time of earthquake occurrence is vital for fixing the location and time of an impending earthquake.

As yet, there has also been no adequate justification with regard to the consistency of PETA manifestations. Previous studies, though limited, have presented conflicting results. For example, the directionality of PETA (i.e. enhancement or depletion) has been linked to time of day, epicentral distance, geographic latitude and orientation of the anomalous electric field (Pulinets et al. 2003; Choi et al. 2012; Hasbi et al. 2011; Yiyan et al. 2009). Furthermore, PETA are detected at different times (i.e. minutes to days and weeks) and do not show systematic correlations with the duration before the earthquake event (see the earlier discussion regarding $n_{pre}$ in Sect. 2.3) (Akhoondzadeh and Saradjian 2011).

Certainly, once the three earthquake prediction parameters (i.e. time, location and strength) are deducible from PETA measurements, ingesting data from multiple sources (i.e. virtual constellation) in a robust observation network would be ideal for the real-time observation and detection of TEC anomalies for earthquake forewarning (Ferretti et al. 2015).

Even though ample ionospheric measurements are available, the locations and earthquake events influence the PETA detection procedure. Since seismically active countries exhibit greater degrees of TEC variability, retrospective case studies conducted in such locations would need to take into account not only background variability (e.g. space weather), but contributions from the regular and smaller-magnitude earthquake events as well. Non-seismically active regions with spatially and temporally isolated earthquake events thus present a more promising opportunity in retrospective analyses. However, for the purpose of earthquake forewarning, this complication could be less important. Earthquakes typically occur closely in time and space, with the main shock generally preceded by smaller-magnitude foreshocks (Jordan et al. 2011). Therefore, detection of the main shock is not imperative, but detection of foreshocks is. This is also valid for earthquake swarms defined by the absence of a clear main shock. As a short-term method, then, the detection of foreshock-related TEC anomalies, in part, gives ample time to decide whether such perturbations are significant enough to issue an earthquake warning. The establishment of $n_{\mathrm{pre}}$ thus becomes a crucial factor in determining the time span of applicability (i.e. interval-of-alarm window) (Jordan et al. 2011). It should be noted that aftershocks are rarely taken into accounted in retrospective studies. Although TEC anomalies may arise both during earthquake preparation (i.e. precursors) and during the main shock and its aftershocks (i.e. co-/post-seismic), aftershocks are seldom the focus in these studies, for two possible reasons: (1) aftershocks are typically weaker and not of primary concern, and, (2) assuming aftershocks similarly cause short-term TEC precursors, existing PETA statistical detection methods are unlikely to register these anomalies, since TEC is already at a perturbed state. Other data processing methodologies may therefore be required for aftershock-related anomalies. For example, recent advances in the area of artificial intelligence, namely deep learning, has seen remarkable success in the prediction of aftershock locations by incorporating in situ ground characteristics such as Coulomb failure stress changes (see DeVries et al. 2018). Nonetheless, more research ought to be directed towards understanding the interactions of TEC levels within the context of the entire seismic sequence.

In the detection of PETA, disparities between values of $N$-day and $Z$ are apparent and often unjustified. Furthermore, the obligatory exclusion of space weather effects appears to be subjective in terms of the indices used and the threshold values. As such, it appears that there are three pertinent issues that need to be resolved:

1. What should the $N$-day and $Z$ be and how should they be decided?
2. How many and which space weather indices should be used?
3. What should the acceptable thresholds for each of these space weather indices be?

In the selection of $N$-day, temporally adjacent earthquakes should be considered. The $N$-day ideally should not cause an overlap with $n_{\mathrm{post}}$ (i.e. period of post-earthquake anomaly) of the previous earthquake, to ensure that only normal ionospheric variations are taken into account. While this condition can be fulfilled in non-seismically active regions, it is challenging for locations which are seismically active, given the frequency of seismic events (where the average recurrence interval is $d$). In an ideal scenario where spatial and temporal confounding effects (i.e. $d \geq 0$) are absent, the range of valid $N$-day values is thus given in Eq. (4), where the maximum value of $N$ (i.e. $N_{\max}$) to capture normal ionospheric variability is $d$:

$$\{N|N \in Z, N \leq d, d \geq 0\}. \tag{4}$$

The exponential scaling relationship between EPZ and earthquake magnitude yields an unrealistically large EPZ radius for large-magnitude earthquakes. While this consequence would seem less impactful on retrospective studies, a large EPZ radius would imply difficulty in establishing a PETA-based earthquake forewarning system. The differences in the nature of earthquake triggers may be correlated against PETA. For example, studies conducted by Astafyeva et al. (2014) and Perevalova et al. (2014) to investigate the link between the degree of TEC anomaly and focal mechanisms (i.e. strike-slip, normal or reverse faults) yielded contrasting results. Therefore, apart from focal mechanisms, future studies on seismic characteristics such as magnitude, relative plate movement rates, on-land vs. submarine events, inter-plate vs. intra-plate events, vertical displacements and hypocenter in relation to the varying nature of PETA are essential to draw crucial earthquake-associated inferences (Jin et al. 2015).

## 4. Conclusion

Currently the feasibility of using PETA in earthquake forewarning is still unclear (Heki and Enomoto 2013). Till now, much effort has been devoted to proving the existence of PETA using various approaches. In this paper, the potential difficulties in implementing PETA for an earthquake forewarning framework based on the current state of knowledge were critically examined. The following issues in the detection of PETA were identified in this study:

1. Differences between ground- and satellite-based PETA observations.
2. Variability of ionospheric TEC in seismically and non-seismically active regions.
3. Spatial and temporal confounding effects from adjacent earthquakes must be considered in analyses.
4. Parameters with arbitrarily defined values ought to be objectively justified or standardized. Those identified in this study include ionospheric shell height, elevation angle, detection confidence (i.e. $Z$), $N$-day and space-related indices.
5. Relevance of the earthquake preparation zone (EPZ) in retrospective and prospective analyses.
6. Lack of research to correlate spatial and temporal PETA variations (e.g. IAZ, $n_{\mathrm{pre}}$) with seismic parameters (e.g. magnitude, epicenter), which is central to establishing time, location and strength for earthquake forewarning.

Although there appears to be strong potential for the use of PETA in earthquake forewarning, the above issues need to be resolved.

*Acknowledgements*

The authors would like to acknowledge the support given by Nanyang Technological University (NTU)–Satellite Research Centre (SaRC) under the project grant (EDB VELOX-CI M4061198.040.70213100) for this study.



## References

Afraimovich, E., Astafieva, E., Gokhberg, M., Lapshin, V., Permyakova, V., Steblov, G., et al. (2004). Variations of the total electron content in the ionosphere from GPS data recorded during the Hector Mine earthquake of October 16, 1999, California. *Russian Journal of Earth Sciences, 6,* 339–354.

Afraimovich, E. L., & Astafyeva, E. I. (2008). TEC anomalies—Local TEC changes prior to earthquakes or TEC response to solar and geomagnetic activity changes? *Earth Planets and Space, 60,* 961–966.

Afraimovich, E., Astafyeva, E., Oinats, A., Yasukevich, Y. V., & Zhivetiev, I. (2008). Global electron content: A new conception to track solar activity. *Annales Geophysicae, 26,* 335–344.

Aggarwal, M. (2015). Anomalous changes in ionospheric TEC during an earthquake event of 13–14 April 2010 in the Chinese sector. *Advances in Space Research, 56,* 1400–1412.

Akhoondzadeh, M. (2013a). An Adaptive Network-based Fuzzy Inference System for the detection of thermal and TEC anomalies around the time of the Varzeghan, Iran, ($M_{\mathrm{w}} = 6.4$) earthquake of 11 August 2012. *Advances in Space Research, 52,* 837–852.

Akhoondzadeh, M. (2013b). Genetic algorithm for TEC seismo-ionospheric anomalies detection around the time of the Solomon ($M_{\mathrm{w}} = 8.0$) earthquake of 06 February 2013. *Advances in Space Research, 52,* 581–590.

Akhoondzadeh, M. (2013c). A MLP neural network as an investigator of TEC time series to detect seismo-ionospheric anomalies. *Advances in Space Research, 51,* 2048–2057.

Akhoondzadeh, M. (2013d). Support vector machines for TEC seismo-ionospheric anomalies detection. *Annales Geophysicae, 31,* 173–186.

Akhoondzadeh, M. (2015). Application of Artificial Bee Colony algorithm in TEC seismo-ionospheric anomalies detection. *Advances in Space Research, 56*(6), 1200–1211.

Anderson, D. L., & Whitcomb, J. H. (1975). Time-dependent seismology. *Journal of Geophysical Research, 80*(11), 1497–1503.

Akhoondzadeh, M., & Saradjian, M. (2011). TEC variations analysis concerning Haiti (January 12, 2010) and Samoa (September 29, 2009) earthquakes. *Advances in Space Research, 47,* 94–104.

Astafyeva, E., Afraimovich, E., Oinats, A., Yasukevich, Y. V., & Zhivetiev, I. (2008). Dynamics of global electron content in 1998–2005 derived from global GPS data and IRI modeling. *Advances in Space Research, 42,* 763–769.

Astafyeva, E., & Heki, K. (2011). Vertical TEC over seismically active region during low solar activity. *Journal of Atmospheric and Solar-Terrestrial Physics, 73,* 1643–1652.

Astafyeva, E., Rolland, L., Lognonné, P., Khelfi, K., & Yahagi, T. (2013). Parameters of seismic source as deduced from 1 Hz ionospheric GPS data: Case study of the 2011 Tohoku-oki event. *Journal of Geophysical Research Space Physics, 118,* 5942–5950.

Astafyeva, E., Rolland, L. M., & Sladen, A. (2014). Strike-slip earthquakes can also be detected in the ionosphere. *Earth and Planetary Science Letters, 405,* 180–193.

Barkat, A., Ali, A., Rehman, K., Awais, M., Tariq, M. A., Ahmed, J., et al. (2018). Multi-precursory analysis of Phalla earthquake (July 2015; $M_w$ 5.1) near Islamabad, Pakistan. *Pure and Applied Geophysics, 2018,* 1–16.

Boughazi, K., Rebouh, S., Aiche, M., & Harkat, N. (2014). Seismic risk and urbanization: The notion of prevention. Case of the city of Algiers. *Procedia Economics and Finance, 18,* 544–551.

Bowman, D., Ouillon, G., Sammis, C., Sornette, A., & Sornette, D. (1998). An observational test of the critical earthquake concept. *Journal of Geophysical Research Solid Earth, 103,* 24359–24372.

Bruevich, E., & Yakunina, G. (2014). Correlation study of six solar activity indices in the cycles 21 ± 23. *Sun and Geosphere, 8,* 83–90.

Calais, E., & Minster, J. B. (1995). GPS detection of ionospheric perturbations following the January 17, 1994, Northridge Earthquake. *Geophysical Research Letters, 22,* 1045–1048.

Carpenter, D. (2004). Remote sensing the Earth's plasmasphere. *Radio Science Bulletin, 308,* 13–29.

Chauhan, V., Singh, O., Kushwah, V., Singh, V., & Singh, B. (2009). Ultra-low-frequency (ULF) and total electron content (TEC) anomalies observed at Agra and their association with regional earthquakes. *Journal of Geodynamics, 48,* 68–74.

Chen, Y.-I., Liu, J.-Y., Tsai, Y.-B., & Chen, C.-S. (2004). Statistical tests for pre-earthquake ionospheric anomaly. *Terrestrial Atmospheric and Oceanic Sciences, 15,* 385–396.

Chmyrev, V., Isaev, N., Serebryakova, O., Sorokin, V., & Sobolev, Y. P. (1997). Small-scale plasma inhomogeneities and correlated ELF emissions in the ionosphere over an earthquake region. *Journal of Atmospheric and Solar-Terrestrial Physics, 59,* 967–974.

Choi, B.-K., & Lee, S. J. (2016). Anomalous ionospheric disturbances over South Korea prior to the 2011 Tohoku earthquake. *Advances in Space Research, 57,* 302–308.

Choi, B., Park, J., & Lee, S. (2012). Ionospheric anomalies observed over South Korea preceding the Great Tohoku earthquake of 2011. *Advances in Space Research, 50,* 311–317.

Ciraolo, L., & Spalla, P. (1999). A statistics of time and space variability of ionospheric electron content at middle latitudes. In: *4th COST 251 Workshop*. Madeira, Portugal.

Clarivate Analytics. (2017). Web of Science product webpage. https://clarivate.com/products/web-of-science/. Accessed 22 Jan 2017.

Contadakis, M.E., Arabelos, D.N., Pikridas, C., & Spatalas, S. (2010). TEC variations over South Europe before and during the M6. 3 Abruzzo earthquake of 6th April 2009. In: *EGU General Assembly Conference Abstracts* (p. 2113).

Contadakis, M., Arabelos, D., Vergos, G., Spatalas, S., & Skordilis, M. (2015). TEC variations over the Mediterranean before and during the strong earthquake ($M = 6.5$) of 12th October 2013 in Crete, Greece. *Physics and Chemistry of the Earth Parts A/B/C, 85,* 9–16.

Dai, X., Liu, J., & Zhang, H. (2015). Application of AR model in the analysis of preearthquake ionospheric anomalies. *Mathematical Problems in Engineering, 2015.*

Dautermann, T., Calais, E., Haase, J., & Garrison, J. (2007). Investigation of ionospheric electron content variations before earthquakes in southern California, 2003–2004. *Journal of Geophysical Research Solid Earth, 112,* B02106.

De Santis, A., De Franceschi, G., Spogli, L., Perrone, L., Alfonsi, L., Qamili, E., et al. (2015). Geospace perturbations induced by the Earth: The state of the art and future trends. *Physics and Chemistry of the Earth Parts A/B/C, 85,* 17–33.

Depueva, A., & Ruzhin, Y. (1993). The equatorial earthquake preparatory stage as a reason of "fountain" effect in the ionosphere. *Preprint IZMIRAN N, 82,* 1029.

Devi, M., Barbara, A., Depueva, A., & Depuev, V. (2008). Preliminary results of TEC measurements in Guwahati, India. *Advances in Space Research, 42,* 753–756.

Devi, M., Barbara, A., Depueva, A., Ruzhin, Y. Y., & Depuev, V. (2010). Anomalous total electron content (TEC) and atmospheric refractivity prior to the very strong China earthquake of May 2008. *International Journal of Remote Sensing, 31,* 3589–3599.

Devi, M., Barbara, A., Oyama, K.-I., & Chen, C.-H. (2014). Earthquake induced dynamics at the ionosphere in presence of magnetic storm. *Advances in Space Research, 53,* 609–618.

DeVries, P. M. R., Viégas, F., Wattenberg, M., & Meade, B. J. (2018). Deep learning of aftershock patterns following large earthquakes. *Nature, 560,* 632–634.

Dieminger, W., Hartmann, G. K., & Leitinger, R. (2012). *The upper atmosphere: Data analysis and interpretation*. Berlin: Springer.

Ding, F., Wan, W., Mao, T., Wang, M., Ning, B., Zhao, B., et al. (2014). Ionospheric response to the shock and acoustic waves excited by the launch of the Shenzhou 10 spacecraft. *Geophysical Research Letters, 41,* 3351–3358.

Dobrovolsky, I., Zubkov, S., & Miachkin, V. (1979). Estimation of the size of earthquake preparation zones. *Pure and Applied Geophysics, 117,* 1025–1044.

Dogan, U., Ergintav, S., Skone, S., Arslan, N., & Oz, D. (2011). Monitoring of the ionosphere TEC variations during the 17th August 1999 Izmit earthquake using GPS data. *Earth Planets and Space, 63,* 1183–1192.

Ferretti, A., Colombo, D., Fumagalli, A., Novali, F., & Rucci, A. (2015). InSAR data for monitoring land subsidence: Time to think big. *Proceedings of the International Association of Hydrological Sciences, 372,* 331–334.

Freund, F. (2000). Time-resolved study of charge generation and propagation in igneous rocks. *Journal of Geophysical Research Solid Earth, 105,* 11001–11019.

Freund, F. T., Kulahci, I. G., Cyr, G., Ling, J., Winnick, M., Tregloan-Reed, J., et al. (2009). Air ionization at rock surfaces and pre-earthquake signals. *Journal of Atmospheric and Solar-Terrestrial Physics, 71,* 1824–1834.

Galvan, D. A., Komjathy, A., Hickey, M. P., Stephens, P., Snively, J., Tony Song, Y., et al. (2012). Ionospheric signatures of

Tohoku-Oki tsunami of March 11, 2011: Model comparisons near the epicenter. *Radio Science, 47,* RS4003.

Guo, J., Li, W., Liu, X., Wang, J., Chang, X., & Zhao, C. (2015). On TEC anomalies as precursor before $M_w$ 8.6 Sumatra earthquake and $M_w$ 6.7 Mexico earthquake on April 11, 2012. *Geosciences Journal, 19,* 721–730.

Guo, J., Yu, H., Li, W., Liu, X., Kong, Q., & Zhao, C. (2016). Total electron content anomalies before $M_w$ 6.0+ earthquakes in the seismic zone of Southwest China between 2001 and 2013. *Journal of Testing and Evaluation, 45,* 131–139.

Hasbi, A. M., Ali, M., & Misran, N. (2011). Ionospheric variations before some large earthquakes over Sumatra. *Natural Hazards and Earth System Sciences, 11,* 597–611.

Hasbi, A.M., Momani, M., Ali, M., & Misran, N. (2009). The relationship between the ionospheric and magnetic disturbances during the 28 March 2005 Sumatran earthquake. In: *Space Science and Communication, 2009. IconSpace 2009. International Conference on* (pp. 166–170): IEEE.

Hayakawa, M., & Molchanov, O. A. (2002). *Seismo-electromagnetics: Lithosphere–atmosphere–ionosphere coupling*. Tokyo: Terra Scientific Publishing Company.

He, L., Wu, L., De Santis, A., Liu, S., & Yang, Y. (2014). Is there a one-to-one correspondence between ionospheric anomalies and large earthquakes along Longmenshan faults? *Annales Geophysicae, 2014,* 187–196.

He, L., Wu, L., Pulinets, S., Liu, S., & Yang, F. (2012). A nonlinear background removal method for seismo-ionospheric anomaly analysis under a complex solar activity scenario: A case study of the M9. 0 Tohoku earthquake. *Advances in Space Research, 50,* 211–220.

Heki, K. (2011). Ionospheric electron enhancement preceding the 2011 Tohoku-Oki earthquake. *Geophysical Research Letters, 38,* L17312.

Heki, K., & Enomoto, Y. (2013). Preseismic ionospheric electron enhancements revisited. *Journal of Geophysical Research Space Physics, 118,* 6618–6626.

Hirooka, S., Hattori, K., Nishihashi, M., Kon, S., & Takeda, T. (2012). Development of ionospheric tomography using neural network and its application to the 2007 Southern Sumatra earthquake. *Electrical Engineering in Japan, 181,* 9–18.

Hocke, K. (2008). Oscillations of global mean TEC. *Journal of Geophysical Research Space Physics, 113,* A04302.

Hsiao, C.-C., Liu, J., Oyama, K.-I., Yen, N., Liou, Y., Chen, S., et al. (2010). Seismo-ionospheric precursor of the 2008 $M_w$7. 9 Wenchuan earthquake observed by FORMOSAT-3/COSMIC. *GPS Solutions, 14,* 83–89.

Hwa, H.Y., & Zain, A.F.M. (2005). Detection of ionospheric perturbation after Northern Sumatra earthquake on 26 December 2004. In, *Applied Electromagnetics, 2005. APACE 2005. Asia-Pacific Conference on* (p. 4 pp.): IEEE.

Islam, M., Sultana, N., Bushra, N., Banna, L., Tusher, T., & Ansary, M. (2015). Effects of earthquake on urbanization in Dhaka City. *Journal of Environmental Science and Natural Resources, 6,* 107–112.

Jhuang, H.-K., Ho, Y.-Y., Kakinami, Y., Liu, J.-Y., Oyama, K.-I., Parrot, M., et al. (2010). Seismo-ionospheric anomalies of the GPS-TEC appear before the 12 May 2008 magnitude 8.0 Wenchuan Earthquake. *International Journal of Remote Sensing, 31,* 3579–3587.

Jiang, W., Ma, Y., Zhou, X., Li, Z., An, X., & Wang, K. (2017). Analysis of ionospheric vertical total electron content before the 1 April 2014 $M_w$ 8.2 Chile earthquake. *Journal of Seismology, 21*(6), 1599–1612.

Jin, S., Occhipinti, G., & Jin, R. (2015). GNSS ionospheric seismology: Recent observation evidences and characteristics. *Earth Science Reviews, 147,* 54–64.

Jing, X., Yiyan, Z., & Yun, W. (2011). Ionospheric VTEC anomalies before Ms7.1 Yushu earthquake. *Geodesy and Geodynamics, 2,* 48–52.

Jordan, T., Chen, Y.-T., Gasparini, P., Madariaga, R., Main, I., Marzocchi, W., et al. (2011). Operational earthquake forecasting: State of knowledge and guidelines for implementation. *Annals of Geophysics, 54,* 4.

Kakinami, Y., Kamogawa, M., Liu, J.-Y., Watanabe, S., & Mogi, T. (2011). Ionospheric disturbance associated with radiation accidents of Fukushima I nuclear power plant damaged by the M9. 0 2011 Tohoku Earthquake. *Advances in Space Research, 48,* 1613–1616.

Kakinami, Y., Yamamoto, M., Chen, C. H., Watanabe, S., Lin, C., Liu, J. Y., et al. (2013). Ionospheric disturbances induced by a missile launched from North Korea on 12 December 2012. *Journal of Geophysical Research Space Physics, 118,* 5184–5189.

Kamogawa, M., & Kakinami, Y. (2013). Is an ionospheric electron enhancement preceding the 2011 Tohoku-Oki earthquake a precursor? *Journal of Geophysical Research Space Physics, 118,* 1751–1754.

Karatay, S., Arikan, F., & Arikan, O. (2010). Investigation of total electron content variability due to seismic and geomagnetic disturbances in the ionosphere. *Radio Science, 45,* RS5012.

Karia, S., & Pathak, K. (2011). Change in refractivity of the atmosphere and large variation in TEC associated with some earthquakes, observed from GPS receiver. *Advances in Space Research, 47,* 867–876.

Karia, S., Sarkar, S., & Pathak, K. (2012). Analysis of GPS-based TEC and electron density by the DEMETER satellite before the Sumatra earthquake on 30 September 2009. *International Journal of Remote Sensing, 33,* 5119–5134.

Karia, S., Sarkar, S., Pathak, K., Sharma, A. K., Ranganath, H., & Gwal, A. K. (2013). Analysis of space-and ground-based parameters prior to an earthquake on 12 December 2009. *International Journal of Remote Sensing, 34,* 7779–7795.

Ke, F., Wang, Y., Wang, X., Qian, H., & Shi, C. (2016). Statistical analysis of seismo-ionospheric anomalies related to Ms $>$ 5.0 earthquakes in China by GPS TEC. *Journal of Seismology, 20,* 137–149.

Klimenko, M., Klimenko, V., Zakharenkova, I., Pulinets, S., Zhao, B., & Tsidilina, M. (2011). Formation mechanism of great positive TEC disturbances prior to Wenchuan earthquake on May 12, 2008. *Advances in Space Research, 48,* 488–499.

Klotz, S., & Johnson, N. (1983). *Encyclopedia of statistical sciences*. Oxford: Wiley.

Komjathy, A., Galvan, D. A., Stephens, P., Butala, M., Akopian, V., Wilson, B., et al. (2012). Detecting ionospheric TEC perturbations caused by natural hazards using a global network of GPS receivers: The Tohoku case study. *Earth Planets and Space, 64,* 1287–1294.

Kon, S., Nishihashi, M., & Hattori, K. (2011). Ionospheric anomalies possibly associated with M$\geqslant$ 6.0 earthquakes in the Japan area during 1998–2010: Case studies and statistical study. *Journal of Asian Earth Sciences, 41,* 410–420.

Kondratenko, A., & Nersesov, I. (1962). Some results of a study of changes in the speeds of longitudinal and transverse waves in the focal zone. *Physics of Earthquakes and Explosion Seismology (in Russian), 25,* 130.

Kouris, S., & Fotiadis, D. (2002). Ionospheric variability: A comparative statistical study. *Advances in Space Research, 29,* 977–985.

Kouris, S., Polimeris, K., & Cander, L. R. (2006). Specifications of TEC variability. *Advances in Space Research, 37,* 983–1004.

Krankowski, A., Zakharenkova, I. E., & Shagimuratov, I. I. (2006). Response of the ionosphere to the Baltic Sea earthquake of 21 September 2004. *Acta Geophysica, 54,* 90–101.

Le, H., Liu, J.-Y., & Liu, L. (2011). A statistical analysis of ionospheric anomalies before 736 M6.0+ earthquakes during 2002–2010. *Journal of Geophysical Research Space Physics, 116,* A02303.

Leyva-Contreras, A., Bisiacchi-Giraldi, G., Pulinets, S., & Ciraolo, L. (2005). Total electron content variations in the ionosphere before the Colima, Mexico, earthquake of 21 January 2003. *Geofisica Internacional, 44,* 369–377.

Li, K., Rollins, J., & Yan, E. (2018). Web of Science use in published research and review papers 1997–2017: A selective, dynamic, cross-domain, content-based analysis. *Scientometrics, 115,* 1–20.

Lin, J.-W. (2010). Two-dimensional ionospheric total electron content map (TEC) seismo-ionospheric anomalies through image processing using principal component analysis. *Advances in Space Research, 45,* 1301–1310.

Lin, J.-W. (2011a). Is it possible to trace an impending earthquake's occurrence from seismo-ionospheric disturbance using principal component analysis? A study of Japan's Iwate-Miyagi Nairiku earthquake on 13 June 2008. *Computers and Geosciences, 37,* 855–860.

Lin, J. (2011b). Seismo-ionospheric disturbance using principal component analysis—a study of Japan's Iwate-Miyagi Nairiku earthquake on 13 June 2008. *Acta Geodaetica et Geophysica Hungarica, 46,* 1–9.

Lin, J.-W. (2013). Ionospheric Anomaly due to the volcanic eruption in Colima, Mexico, 06 January 2013: Two-dimensional principal component analysis. *European Journal of Remote Sensing, 46,* 689–698.

Liperovsky, V., Pokhotelov, O., Liperovskaya, E., Parrot, M., Meister, C.-V., & Alimov, O. (2000). Modification of sporadic E-layers caused by seismic activity. *Surveys In Geophysics, 21,* 449–486.

Liu, J., Chen, C., Chen, Y., Yang, W., Oyama, K., & Kuo, K. (2010a). A statistical study of ionospheric earthquake precursors monitored by using equatorial ionization anomaly of GPS TEC in Taiwan during 2001–2007. *Journal of Asian Earth Sciences, 39,* 76–80.

Liu, J.-Y., Chen, Y., Chuo, Y., & Chen, C.-S. (2006a). A statistical investigation of preearthquake ionospheric anomaly. *Journal of Geophysical Research Space Physics, 111,* A05304.

Liu, J., Chen, Y., Chuo, Y., & Tsai, H. (2001). Variations of ionospheric total electron content during the Chi–Chi earthquake. *Geophysical Research Letters, 28,* 1383–1386.

Liu, L., Chen, Y., Le, H., Kurkin, V. I., Polekh, N. M., & Lee, C. C. (2011). The ionosphere under extremely prolonged low solar activity. *Journal of Geophysical Research Space Physics, 116,* A04320.

Liu, J. Y., Chuo, Y. J., Shan, S. J., Tsai, Y. B., Pulinets, S. A., & Yu, S. B. (2004). Pre-earthquake ionospheric anomalies monitored by GPS TEC. *Annales Geophysicae, 22,* 1585–1593.

Liu, J., Lin, C., Chen, Y., Lin, Y., Fang, T., Chen, C., et al. (2006b). Solar flare signatures of the ionospheric GPS total electron content. *Journal of Geophysical Research Space Physics, 111,* A05308.

Liu, W., & Xu, L. (2017). Statistical analysis of ionospheric TEC anomalies before global $M_w \geq 70$ earthquakes using data of CODE GIM. *Journal of Seismology, 21*(4), 759–775.

Liu, J. Y., Chen, Y. I., Chen, C. H., & Hattori, K. (2010b). Temporal and spatial precursors in the ionospheric global positioning system (GPS) total electron content observed before the 26 December 2004 M93 Sumatra-Andaman Earthquake. *Journal of Geophysical Research Space Physics, 115,* 312.

Mareev, E., Iudin, D., & Molchanov, O. (2002). Mosaic source of internal gravity waves associated with seismic activity. In M. Hayakawa (Ed.), *Seismo-electromagnetics: Lithosphere–atmosphere–ionosphere coupling* (pp. 335–342). Tokyo: Terra Scientific Publishing Company.

Masci, F. (2012). The study of ionospheric anomalies in Japan area during 1998–2010 by Kon et al.: An inaccurate claim of earthquake-related signatures? *Journal of Asian Earth Sciences, 57,* 1–5.

Masci, F. (2013). Further comments on the ionospheric precursor of the 1999 Hector Mine earthquake. *Natural Hazards and Earth System Sciences, 13,* 193–196.

Masci, F., & Thomas, J. N. (2014). Comment on "Temporal and spatial precursors in ionospheric total electron content of the 16 October 1999 $M_w$ 7.1 Hector Mine earthquake" by Su et al. (2013). *Journal of Geophysical Research Space Physics, 119,* 6994–6997.

Masci, F., & Thomas, J. (2015). On the reliability of the Spatial Scintillation Index to detect earthquake precursors in the ionosphere. *Radio Science, 50,* 745–753.

Masci, F., Thomas, J. N., & Secan, J. A. (2017). On a reported effect in ionospheric TEC around the time of the 6 April 2009 L'Aquila earthquake. *Natural Hazards and Earth Systems Sciences, 17,* 1461–1468.

Masci, F., Thomas, J. N., Villani, F., Secan, J. A., & Rivera, N. (2015). On the onset of ionospheric precursors 40 min before strong earthquakes. *Journal of Geophysical Research Space Physics, 120,* 1383–1393.

Mazzella, A. J. (2009). Plasmasphere effects for GPS TEC measurements in North America. *Radio Science, 44,* RS5014.

Mendillo, M., Huang, C.-L., Pi, X., Rishbeth, H., & Meier, R. (2005). The global ionospheric asymmetry in total electron content. *Journal of Atmospheric and Solar Terrestrial Physics, 67,* 1377–1387.

Molchanov, O., & Hayakawa, M. (1995). Generation of ULF electromagnetic emissions by microfracturing. *Geophysical Research Letters, 22,* 3091–3094.

Molchanov, O., & Hayakawa, M. (1998). On the generation mechanism of ULF seismogenic electromagnetic emissions. *Physics of the Earth and Planetary Interiors, 105,* 201–210.

Monroe, J. S., Wicander, R., & Hazlett, R. W. (2007). *Physical geology: Exploring the Earth* (p. c2007). Belmont: Thomson Brooks/Cole.

Moore, G.W. (1964). Magnetic *disturbances preceding* the 1964 Alaska *earthquake*, pp. 508–509.

Mukhtarov, P., Pancheva, D., Andonov, B., & Pashova, L. (2013). Global TEC maps based on GNSS data: 1. Empirical background TEC model. *Journal of Geophysical Research Space Physics, 118,* 4594–4608.

Namgaladze, A., Klimenko, M., Klimenko, V., & Zakharenkova, I. (2009). Physical mechanism and mathematical modeling of earthquake ionospheric precursors registered in total electron content. *Geomagnetism and Aeronomy, 49,* 252–262.

Natali, M. P., & Meza, A. (2011). Annual and semiannual variations of vertical total electron content during high solar activity based on GPS observations. *Annales Geophysicae, 29,* 865–873.

Nenovski, P., Pezzopane, M., Ciraolo, L., Vellante, M., Villante, U., & De Lauretis, M. (2015). Local changes in the total electron content immediately before the 2009 Abruzzo earthquake. *Advances in Space Research, 55,* 243–258.

Perevalova, N., Sankov, V., Astafyeva, E., & Zhupityaeva, A. (2014). Threshold magnitude for ionospheric TEC response to earthquakes. *Journal of Atmospheric and Solar Terrestrial Physics, 108,* 77–90.

Ping, J., Matsumoto, K., Heki, K., Saito, A., Callahan, P., Potts, L., et al. (2004). Validation of Jason-1 nadir ionosphere TEC using GEONET. *Marine Geodesy, 27,* 741–752.

Plotkin, V. (2003). GPS detection of ionospheric perturbation before the 13 February 2001, El Salvador earthquake. *Natural Hazards and Earth System Science, 3,* 249–253.

Polyakov, Y. S., Ryabinin, G. V., Solovyeva, A. B., & Timashev, S. F. (2015). Is it possible to predict strong earthquakes? *Pure and Applied Geophysics, 172,* 1945–1957.

Pulinets, S. (2004). Ionospheric precursors of earthquakes; recent advances in theory and practical applications. *Terrestrial Atmospheric and Oceanic Sciences, 15,* 413–436.

Pulinets, S., & Boyarchuk, K. (2004). *Ionospheric precursors of earthquakes*. Berlin: Springer.

Pulinets, S., Kotsarenko, A., Ciraolo, L., & Pulinets, I. (2007). Special case of ionospheric day-to-day variability associated with earthquake preparation. *Advances in Space Research, 39,* 970–977.

Pulinets, S., Legen'Ka, A., Gaivoronskaya, T., & Depuev, V. K. (2003). Main phenomenological features of ionospheric precursors of strong earthquakes. *Journal of Atmospheric and Solar Terrestrial Physics, 65,* 1337–1347.

Pulinets, S., & Ouzounov, D. (2011). Lithosphere–Atmosphere–Ionosphere Coupling (LAIC) model—an unified concept for earthquake precursors validation. *Journal of Asian Earth Sciences, 41,* 371–382.

Pundhir, D., Singh, B., & Singh, O. (2014). Anomalous TEC variations associated with the strong Pakistan–Iran border region earthquake of 16 April 2013 at a low latitude station Agra, India. *Advances in Space Research, 53,* 226–232.

Reddy, C. D., Shrivastava, M. N., Seemala, G. K., González, G., & Baez, J. C. (2016). Ionospheric plasma response to $M_w$ 8.3 Chile Illapel earthquake on September 16, 2015. *Pure and Applied Geophysics, 173,* 1451–1461.

Rikitake, T. (1969). An approach to prediction of magnitude and occurrence time of earthquakes. *Tectonophysics, 8,* 81–95.

Rikitake, T. (1975). Dilatancy model and empirical formulas for an earthquake area. *Pure and Applied Geophysics, 113,* 141–147.

Rishbeth, H. (2006). Ionoquakes: Earthquake precursors in the ionosphere? *Eos Transactions American Geophysical Union, 87,* 316.

Saba, M. F., Gonzalez, W., & Clúa de Gonzalez, A. (1997). Relationships between the AE, ap and Dst indices near solar minimum (1974) and at solar maximum (1979). *Annales Geophysicae, 15,* 1265–1270.

Sánchez-Dulcet, F., Rodríguez-Bouza, M., Silva, H., Herraiz, M., Bezzeghoud, M., & Biagi, P. (2015). Analysis of observations backing up the existence of VLF and ionospheric TEC anomalies before the $M_w$6. 1 earthquake in Greece, January 26, 2014. *Physics and Chemistry of the Earth Parts A/B/C, 85,* 150–166.

Sarkar, S., & Gwal, A. (2010). Satellite monitoring of anomalous effects in the ionosphere related to the great Wenchuan earthquake of May 12, 2008. *Natural Hazards, 55,* 321–332.

Savitzky, A., & Golay, M. J. (1964). Smoothing and differentiation of data by simplified least squares procedures. *Analytical Chemistry, 36,* 1627–1639.

She, C., Wan, W., Yue, X., Xiong, B., Yu, Y., Ding, F., et al. (2017). Global ionospheric electron density estimation based on multisource TEC data assimilation. *GPS Solutions, 21,* 1125–1137.

Singh, O., Chauhan, V., Singh, V., & Singh, B. (2009). Anomalous variation in total electron content (TEC) associated with earthquakes in India during September 2006–November 2007. *Physics and Chemistry of the Earth Parts A/B/C, 34,* 479–484.

Šlégr, J., & Váňová, K. (2017). Stochastic properties of lower ionosphere as earthquake precursor. *Journal of Seismology, 21,* 243–248.

Sompotan, A. F., Puspito, N. T., Joelianto, E., & Hattori, K. (2015). Analysis of ionospheric precursor of earthquake using GIM-TEC, Kriging and neural network. *Asian Journal of Earth Sciences, 8,* 32–44.

Surkov, V. (1999). ULF electromagnetic perturbations resulting from the fracture and dilatancy in the earthquake preparation zone. In M. Hayakawa (Ed.), *Atmospheric and ionospheric phenomena associated with earthquakes* (pp. 357–370). Tokyo: Terrapub.

Surkov, V., Molchanov, O., & Hayakawa, M. (2003). Pre-earthquake ULF electromagnetic perturbations as a result of inductive seismomagnetic phenomena during microfracturing. *Journal of Atmospheric and Solar Terrestrial Physics, 65,* 31–46.

Thomas, J., Huard, J., & Masci, F. (2017). A statistical study of global ionospheric map total electron content changes prior to occurrences of M $\geq$ 6.0 earthquakes during 2000–2014. *Journal of Geophysical Research Space Physics, 122,* 2151–2161.

Thomas, J. N., Love, J. J., Komjathy, A., Verkhoglyadova, O. P., Butala, M., & Rivera, N. (2012). On the reported ionospheric precursor of the 1999 Hector Mine, California earthquake. *Geophysical Research Letters, 39,* L06302.

Tojiev, S., Ahmedov, B., Tillayev, Y., & Eshkuvatov, H. (2013). Ionospheric anomalies of local earthquakes detected by GPS TEC measurements using data from Tashkent and Kitab stations. *Advances in Space Research, 52,* 1146–1154.

Tong, W.K. (1988). *Abnormal Animal Behavior and the Prediction of Earthquakes*. Master Thesis, Dept. Earth Sciences, Northeastern Illinois University.

Trigunait, A., Parrot, M., Pulinets, S., & Li, F. (2004). Variations of the ionospheric electron density during the Bhuj seismic event. *Annales Geophysicae, 22,* 4123–4131.

Tsai, Y.-B., Liu, J.-Y., Ma, K.-F., Yen, H.-Y., Chen, K., Chen, Y., et al. (2004). Preliminary results of the iSTEP program on integrated search for Taiwan earthquake precursors. *Terrestrial Atmospheric and Oceanic Sciences, 15,* 545–562.

Ulukavak, M., & Yalcinkaya, M. (2016). Precursor analysis of ionospheric GPS-TEC variations before the 2010 M7.2 Baja California earthquake. *Geomatics Natural Hazards and Risk, 8,* 295–308.

Wu, M., Guo, P., Xu, T., Fu, N., Xu, X., Jin, H., et al. (2015). Data assimilation of plasmasphere and upper ionosphere using COSMIC/GPS slant TEC measurements. *Radio Science, 50,* 1131–1140.

Xu, G., Han, P., Huang, Q., Hattori, K., Febriani, F., & Yamaguchi, H. (2013). Anomalous behaviors of geomagnetic diurnal variations prior to the 2011 off the Pacific coast of Tohoku earthquake ($M_w$ 9.0). *Journal of Asian Earth Sciences, 77,* 59–65.

Xu, T., Hu, Y., Wu, J., Wu, Z., Suo, Y., Feng, J., et al. (2010). Abnormal perturbations in the ionospheric F2 region before Wenchuan earthquake on 12 May 2008. *Science China Earth Sciences, 53,* 1671–1674.

Yiyan, Z., Yun, W., Xuejun, Q., & Xunxie, Z. (2009). Ionospheric anomalies detected by ground-based GPS before the $M_w$ 7. 9 Wenchuan earthquake of May 12, 2008, China. *Journal of Atmospheric and Solar Terrestrial Physics, 71,* 959–966.

Yu, T., Mao, T., Wang, Y., & Wang, J. (2009). Study of the ionospheric anomaly before the Wenchuan earthquake. *Chinese Science Bulletin, 54,* 1080–1086.

Zakharenkova, I., Astafyeva, E., & Cherniak, I. (2016). GPS and in situ Swarm observations of the equatorial plasma density irregularities in the topside ionosphere. *Earth Planets and Space, 68,* 1–11.

Zakharenkova, I., Shagimuratov, I., Tepenitzina, N. Y., & Krankowski, A. (2008). Anomalous modification of the ionospheric total electron content prior to the 26 September 2005 Peru earthquake. *Journal of Atmospheric and Solar Terrestrial Physics, 70,* 1919–1928.

Zhang, X., Shen, X., Liu, J., Ouyang, X., Qian, J., & Zhao, S. (2009). Analysis of ionospheric plasma perturbations before Wenchuan earthquake. *Natural Hazards and Earth System Science, 9,* 1259–1266.

Zhu, F., Su, F., & Lin, J. (2018). Statistical analysis of TEC anomalies prior to M6.0+ earthquakes during 2003–2014. *Pure and Applied Geophysics, 175,* 3441–3450.

(Received September 1, 2018, revised December 3, 2018, accepted December 20, 2018, Published online January 3, 2019)